Quantum Optics and Quantum Information Processing in Rare-Earth-Ion-Doped Crystals

Ohlsson, Nicklas

2003

Quantum Optics and Quantum Information Processing in Rare-Earth-Ion-Doped Crystals

Nicklas Ohlsson

Lund Reports on Atomic Physics
LRAP-300

Doctoral Thesis
Department of Physics
Lund Institute of Technology
April 2003

ISBN 91-628-5645-6

Table of contents

Abstract

In this thesis, aspects of the use of cryogenically cooled rare-earth-ion-doped crystals in the fields of quantum optics and quantum information processing are addressed. The experiments and theoretical considerations referred to in this thesis are based on the coherent transient interaction between light and the ions in the crystals.

A photon echo experiment has been performed where faint optical pulses were accumulated in the crystal. In this experiment, the possibility of single photons acting as two of the optical fields in the photon echo process was investigated. Different aspects on the experiment, which can be viewed as delayed self-interference of a single photon, are discussed in this thesis.

A scheme for the possible implementation of quantum information processing in rare-earth-ion-doped crystals is presented. A key feature in this scheme is that small groups of ions, which can be optically manipulated and which interact in a controlled way, can be extracted from a collection of randomly positioned ions in the crystal host. Initial experimental investigations of the scheme, indicating the possibility of implementing quantum gates, are also presented in this thesis.

In another experiment, the application of magnetic fields of up to 5 T was seen to increase the lifetime of information stored as frequency-dependent modulation of the population of thulium ions doped into a YAG crystal by several orders of magnitude. This mechanism might be useful in data storage and information processing applications. An experiment in which the same type of crystal was used as the active medium in a photon-echo-based pulse compression experiment, where microsecond long pulses were compressed to nanosecond duration using frequency-chirped light pulses, is also reported in this thesis.

Sammanfattning

Ljusets minsta kända beståndsdelar kallas fotoner. Enligt kvantmekaniken har dessa egenskaper som normalt förknippas med vågor och samtidigt sådana egenskaper som normalt förknippas med partiklar. Partikelegenskaperna tar sig uttryck i att den minsta mängd ljus som går att mäta är den mängd som motsvaras av en foton. Vågegenskaperna, å andra sidan, visar sig i interferensexperiment, där en enskild foton verkar kunna ta två olika vägar samtidigt för att sedan kunna interferera med sig själv. Denna dualism mellan våg- och partikelnaturen hos fotoner har studerats flitigt under de senaste hundra åren.

I denna avhandling presenteras ett experiment, där enskilda fotoner har fått växelverka med joner indopade i en kristall. Experimentet indikerar att enskilda fotoner kan delas upp i två pulser som absorberas av jonerna i kristallen. Sedan absorptionen av många enskilda fotoner ackumulerats i kristallen är det möjligt att få information om tidsskillnaden mellan de två pulserna. Detta trots att en direkt mätning av pulserna skulle visa att fotonerna befann sig i antingen den ena pulsen eller den andra, men aldrig i båda samtidigt. Vid en sådan mätning skulle det vara omöjligt att få information om tiden mellan pulserna. Experimentet som presenteras i avhandlingen kan tolkas som att de båda pulserna interfererar med varandra i kristallen trots att de aldrig befinner sig där samtidigt.

En annan del av avhandlingen behandlar området kvantdatorer. Dagens datorer behandlar information i form av bitar som kan ha antingen värdet ett eller värdet noll. I en kvantdator representeras bitarna, vilka kallas kvantbitar, av kvantmekaniska system. Detta innebär att kvantbitarna kan anta värdena noll och ett, precis som bitarna i en vanlig dator, men att de även kan vara i en superposition av de båda värdena. Detta gör att datorn kan räkna på båda de möjliga värdena parallellt, vilket gör det möjligt att utföra vissa typer av beräkningar snabbare än om en vanlig dator hade använts. Byggandet av kvantdatorer befinner sig fortfarande på experimentstadiet och ett stort antal fysikaliska system, som föreslagits som möjliga för att implementera kvantdatorberäkningar, undersöks för närvarande.

Inom ramen för denna avhandling har möjligheten att utföra elementära kvantdatorberäkningar med hjälp av kristaller dopade med joner från de sällsynta jordartsmetallerna undersökts. I avhandlingen presenteras ett förslag på hur detta skulle kunna göras. Förslaget går ut på att låta joner som absorberar ljus med olika våglängd utgöra olika kvantbitar. För att kunna använda kvantbitarna i logiska grindar krävs det att jonerna i de olika kvantbitarna kan växelverka med varandra. Ett tillvägagångssätt för att från en kristall välja ut endast de joner där denna växelverkan är tillräckligt stark har också utvecklats och presenteras i avhandlingen. Vidare har experiment utförts för att undersöka om förslaget går att realisera i praktiken.

Slutligen har samma typ av kristaller som de ovan beskrivna använts för att komprimera optiska pulser. Genom att använda en optisk process kallad fotonekon, kunde optiska pulser, ursprungligen mikrosekunder långa, komprimeras till längder i nanosekundsområdet. Samma typ av kristaller har

också undersökts då de placerats i ett starkt magnetfält. Detta visade sig ge upphov till en mekanism för långtidslagring av information i kristallen, vilket kan ha tillämpningar inom optisk datalagring och signalbehandling.

List of papers

This thesis is based on the following papers:

Paper I

X. J. Wang, M. Afzelius, N. Ohlsson, U. Gustafsson, and S. Kröll, "Coherent transient data-rate conversion and data transformation", Opt. Lett. **25**, 945 (2000)

Paper II

N. Ohlsson, M. Nilsson, R. K. Mohan, and S. Kröll, "Long-time storage mechanism for Tm:YAG in a magnetic field", Opt. Lett. **28**, 450 (2003).

Paper III

N. Ohlsson, M. Nilsson, and S. Kröll, "Experimental investigation of delayed self-interference for single photons", Submitted to Phys. Rev. A, December (2002).

Paper IV

N. Ohlsson, R.K. Mohan, and S. Kröll, "Quantum computer hardware based on rare-earth-ion-doped inorganic crystals", Optics Commun. **201**, 71 (2002).

Paper V

M. Nilsson, L. Rippe, N. Ohlsson, T. Christiansson, and S. Kröll, "Initial experiments concerning quantum information processing in rare-earth-ion doped crystals", Physica Scripta **T102**, 178 (2002)

1. Introduction

The realisation of the laser in 1960 opened up the possibility of studying coherent interactions between light and atoms.[1] This thesis deals with phenomena arising when coherent pulses of light interact with a collection of ions doped into an inorganic crystal, where each ion only absorbs light within a narrow frequency band, but the different ions in the crystal absorb at different frequencies. In order to study controlled interactions between laser light and the ions in the crystal, the samples have been placed in a cryostat and cooled to liquid helium temperature (~ 4 K). At such a low temperature, uncontrollable interactions with the environment (e.g. in the form of phonons) are minimised, enabling well-controlled optical manipulation of the state of the ions. In this work, the ability of the ions to store the phase of the electromagnetic field has been studied in different experiments.

During the past two decades, research on coherent interactions between light and rare-earth-ion-doped crystals at cryogenic temperatures has mainly been in the area of all-optical data storage and signal processing. In this work, (as in other studies during recent years) attention has turned towards the use of the same type of materials for performing fundamental experiments in quantum physics and for exploring the new and exciting field of quantum information processing. The quest to reveal the secrets of quantum physics spurs the development of better lasers, crystals and other equipment, which will most certainly also have a positive effect on more applied areas of research.

In this work, a quantum optical experiment involving accumulated photon echoes has been studied. The study of quantum optical experiments can lead to a better understanding of the properties of light, but also of the nature of various types of optical processes. In the accumulated photon echo experiment (also called *delayed single-photon self-interference*), a large number of pulse pairs, each containing on average less than one photon, were made to interact with a rare-earth-ion-doped crystal. The experiment supported the suggestion that the non-linear photon echo process can be performed with only a single photon shared between the first two optical pulses.

During this work, I have also been given the opportunity to work in the rather new research field of quantum information processing. In this field, the combination of quantum physics and information theory has revealed possibilities for computations with fewer computational steps than intuitively believed to be

possible.[2,3] This field has, in my opinion, changed the way we think about computations in a significant way. Until recently, it was assumed that the exact physical implementation of a machine capable of performing calculations was not of great importance. This assumption has made it possible to develop algorithms without worrying about the details of the machine on which the algorithms were to be implemented. However, there are strong indications that clever usage of a computational machine in which quantum mechanics is utilised can solve some problems significantly faster than a device based on classical physics. In this thesis, a suggestion for a possible way of performing quantum information processing in rare-earth-ion-doped crystals is presented together with initial experiment towards the implementation of elementary computations.

This thesis is divided into two parts. The first part contains some background information relevant for the study of coherent interactions between light and rare-earth ions doped into crystals, and the second part contains the scientific papers on which this thesis is based. In Chapter 2 of the first part, the theory of coherent interactions between light and atoms is summarised. In Chapter 3, a description of some of the special optical properties possessed by rare-earth-ion-doped crystals is given. Chapter 4 contains an explanation of the photon echo process and some practical applications in which the use of photon echoes has been envisaged. In Chapter 5, some issues relevant for the delayed single-photon self-interference experiment (reported in Paper III) are elaborated upon. Chapter 6 contains a description of the mysteries of quantum information processing and the possibility of performing such processing in the rare-earth-ion-doped crystals. The survey of theoretical and experimental considerations in the first part of this thesis is by no means complete, but is rather a summary of the phenomena that I personally have found most enlightening or puzzling.

2. Coherent interaction between light and atoms

In this section, the coherent interaction between light and an ensemble of atoms will be described. The interaction will be assumed to only involve one optical transition of the atoms, i.e. the atoms will be approximated by two-level systems. The theory presented is semi-classical in that the light is described as a continuous classical electromagnetic field rather than a quantised field consisting of photons. Some effects related to the quantisation of the electromagnetic field will be described in Chapter 5 of this thesis. Derivations of the equations describing the interaction between coherent light and two-level atoms can be found in many text-books, see e.g. References 4-6. In this chapter, some of the equations will be repeated and briefly commented upon to give a theoretical background for the following chapters in the thesis.

2.1. Two-level atoms

Atoms can, in general, exist in infinitely many stationary energy states. A full description of the interaction between light and all the energy levels of an atom would be very complicated. However, if a monochromatic light source is used where the frequency of the light is tuned so as to be close to the energy difference between only two of the energy levels of the atom, the description can be simplified considerably. The assumption that only two energy levels are involved in the interaction between light and atoms is not valid for all the experiments described in this thesis, but an understanding of this simple case can be useful when considering more complicated processes.

An atom with two energy levels will, after a measurement, be found in one of its two levels, but if no measurement is made, it can exist in a coherent superposition of the two states. For an atom with two levels (ground and excited state), denoted |g> and |e>, a general state can be described as:

$$|\psi(t)>= c_g(t)\,|g> + c_e(t)e^{-i\omega_{eg}t}\,|e>, \qquad (2.1)$$

where ω_{eg} is the frequency corresponding to the energy difference between the levels. c_g and c_e are the complex amplitudes of the ground and excited states. The square modulus of these amplitudes describes the probability of measuring the atom in each state, and consequently:

$$|c_g(t)|^2 + |c_e(t)|^2 = 1 \tag{2.2}$$

must hold at all times. As can be seen in Equation 2.1 above, an atom in a superposition between its two states will have a phase factor evolving with the absorption frequency of the transition between the two states. It is interesting to note that an equal superposition between energy states is mathematically very similar to the state of e.g. a photon, after a 50/50 beamsplitter, which is a common example used for illustrating the peculiarities of superpositions in quantum mechanics. This similarity will be further commented upon in Chapter 5. The time during which an atom evolving freely in a superposition between two states can oscillate at its transition frequency without any perturbation is given by the phase memory time, T_2, of the atom. This time is limited by the lifetimes of the two atomic energy levels, but is often much shorter due to interactions with the environment. Such interactions could take the form of phase perturbing collisions for atoms in gases or may be interactions with phonons for ions in solid state hosts. In this chapter, this time (T_2) will be assumed to be much longer than the duration of the interaction between the atom and the light, but in the following chapters of this thesis the phase memory time will require careful consideration.

A monochromatic (linearly polarised) laser field can, in the dipole approximation, be described as:

$$E(t) = E_0 \cos\omega t\,, \tag{2.3}$$

where E_0 is the amplitude and ω is the frequency of the field. For a laser to produce this field, the coherence time of the laser would have to be infinitely long. This is not possible in practice, but the description is still valid if the duration of the interaction between light and atoms is shorter than the coherence time of the laser used in the experiment. The interaction between this field and atoms can be described by:

$$\begin{aligned} V(t) &= -\mu_{eg} E(t), \\ H &= H_0 + V(t), \end{aligned} \tag{2.4}$$

where H_0 is the Hamiltonian describing the unperturbed atom, resulting in the energy levels of the atom, and V describes the coupling between the field and the atoms. The coupling strength between the field and the atoms is described by the atomic transition dipole moment, μ_{eg}. Inserting this into the Schrödinger equation makes it possible to follow the dynamics of the atoms in the field:

$$i\hbar \frac{\partial |\psi(t)>}{\partial t} = H |\psi(t)> . \tag{2.5}$$

It is convenient to introduce some new variables to describe the dynamics of the atomic state. Physical interpretations of these will be given later in this chapter. The Rabi frequency, Ω, is given by:

$$\Omega = \frac{|\mu_{eg}| E_0}{\hbar} . \tag{2.6}$$

The detuning between the frequency of the light field and the atomic absorption frequency is denoted Δ:

$$\Delta = \omega_{eg} - \omega . \tag{2.7}$$

Further, the generalised Rabi frequency, Ω_G, is given by:

$$\Omega_G = \sqrt{\Omega^2 + \Delta^2} . \tag{2.8}$$

Solving the Schrödinger equation for this type of atomic state (in the rotating wave approximation) gives the solutions[4]:

$$\begin{aligned} c_g(t) &= \left\{ \begin{array}{l} c_g(0)\left[\cos\left(\frac{\Omega_G t}{2}\right) - \frac{i\Delta}{\Omega_G}\sin\left(\frac{\Omega_G t}{2}\right)\right] + \\ + i\frac{\Omega}{\Omega_G} c_e(0)\sin\left(\frac{\Omega_G t}{2}\right) \end{array} \right\} e^{i\Delta t/2} \\ c_e(t) &= \left\{ \begin{array}{l} c_e(0)\left[\cos\left(\frac{\Omega_G t}{2}\right) + \frac{i\Delta}{\Omega_G}\sin\left(\frac{\Omega_G t}{2}\right)\right] + \\ + i\frac{\Omega}{\Omega_G} c_g(0)\sin\left(\frac{\Omega_G t}{2}\right) \end{array} \right\} e^{-i\Delta t/2} \end{aligned} \tag{2.9}$$

A simple special case is if we assume that the atom is initially in its ground state, i.e. that $c_g(0)=1$ and $c_e(0)=0$, and that the field is resonant with the atomic transition frequency. The solutions above then simplify to:

$$\begin{aligned} c_g(t) &= \cos\frac{\Omega t}{2}, \\ c_e(t) &= i\sin\frac{\Omega t}{2}, \end{aligned} \tag{2.10}$$

which means that a resonant field will drive the atoms from the ground state to the excited state and then back again. A full period of this oscillation between the two states (given by the square of the amplitudes) will have been executed when $\Omega \cdot t = 2\pi$, see Figure 1. These oscillations are called Rabi oscillations and Ω, as mentioned above, is the Rabi frequency, which describes the rate at which the transfer between the states is taking place. The product of the Rabi frequency and the interaction time between the light and the atom will determine the effect of the field on the atomic state. This product is commonly referred to as the pulse area.[7] A pulse that can transfer the atom from its ground state to an equal superposition between the two states is therefore called a $\pi/2$ pulse, a pulse that transfers the same atom completely to the excited state is a π pulse, and so on.

For an atom where the detuning between the electromagnetic field and the atomic absorption frequency is non-zero, the atom will never be completely transferred into the excited state. The probability of finding the atom in the excited state will first increase, as a function of time, but before reaching a value of unity, the probability will again start to decrease. The oscillations in this case will take place on a shorter time-scale than for the case of a resonant atom, and is described by the generalised Rabi frequency, see Equation 2.8 and Figure 1.

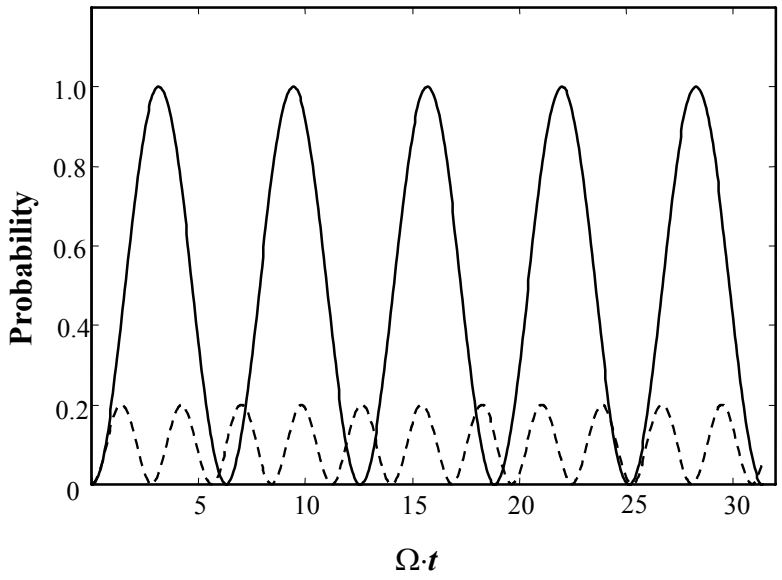

Figure 1. Rabi oscillations for an atom in resonance with an applied electromagnetic field (solid line) and for an atom with a detuning of $\Delta = 2*\Omega$ (dashed line). The y-axis shows the probability of finding the atom in the excited state, and the x-axis gives the interaction time between a coherent light field and the atom.

2.2. The Bloch vector model

A common way to describe and visualise the evolution of a quantum mechanical two-level system is to use the Bloch sphere. In this model, a different set of variables from those in Section 2.1 is used to describe the state of the two-level atom. First, a new variable describing the probability of finding the atom in each state is introduced:

$$w(t) = \left|c_e(t)\right|^2 - \left|c_g(t)\right|^2, \tag{2.11}$$

where w is called the inversion, taking a value of -1 when the atom is in its ground state, and a value of $+1$ when it is in its excited state. Further, variables describing the phase of the atomic state compared to that of the electromagnetic field are introduced as:

$$2 \cdot c_g(t) \cdot c_e(t)^* = u(t) - iv(t), \tag{2.12}$$

where u describes the part of the atomic state that oscillates with the same phase as the applied electromagnetic field (see Equation 2.3), and v is the part that oscillates with a phase difference of 90° with respect to the electromagnetic field. The variables are normalised according to Equations 2.11 and 2.12 so that:

$$w^2 + u^2 + v^2 = 1. \tag{2.13}$$

Using these variables the possible states of the atom can thus be visualised as points on a unit sphere, called the Bloch sphere, in the w, u and v coordinate system, see Figure 2.

For an atom in the ground state, w will be equal to -1 and u and v will both be zero, which reflects the stationary nature of the energy eigenstates of the atom. This state can then be described by a (Bloch) vector pointing from the origin of the Bloch sphere along the w-axis, see Figure 2. When a resonant optical field is applied to this atom, the state of the atom will change according to Equation 2.10. In the Bloch sphere this change can be visualised as a movement of the Bloch vector on the sphere in the vw-plane. As an example, a $\pi/2$ pulse will transfer the atom to a state described by a unit vector along the v-axis. The action of resonant pulses can, in the Bloch vector model, be described as rotations around a pseudo-vector, representing the laser field, pointing along the u-axis. This pseudo-vector can also be used to describe the action of non-resonant pulses. In this case, the pseudo-vector will not point along the u-axis, but will be in the uw-plane, at an angle to the u-axis that reflects the detuning between the field and the atomic frequency, see Figure 3. As before, the action of the applied field on the atom is described by rotation of the Bloch vector around the pseudo-vector.

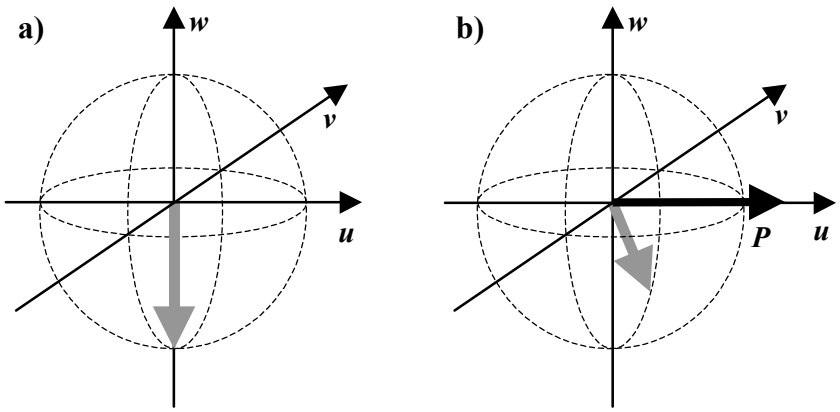

Figure 2. A two-level system can be represented by a Bloch vector in a Bloch-sphere. a) An atom in the ground state is represented by a Bloch vector pointing downwards along the w-axis. b) interaction with a resonant electromagnetic field rotates the Bloch vector around a pseudo vector, P, pointing along the positive u-axis.

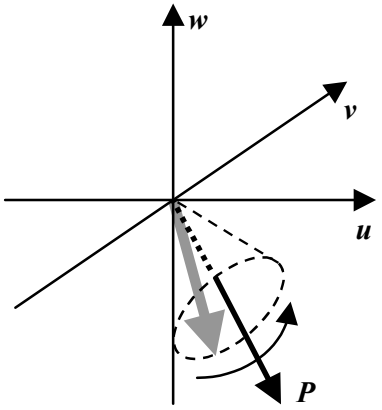

Figure 3. For a non-resonant electromagnetic field, the pseudo vector, P, representing the field will have an angle to the u-axis, and the Bloch vector will rotate around this vector.

An atom in a superposition state will act as a small electric dipole oscillating at the transition frequency of the atom. The variables *u* and *v* are proportional to the polarisation which oscillates in and 90° out of phase with the applied field. According to Maxwell's equations, an oscillating dipole will, emit light with a frequency corresponding to the oscillation frequency of the dipole. This light will be radiated 90° out of phase with the polarisation. This means that an atom that is transferred from the ground state to the excited state will emit light that is 180° out of phase with the applied light field. The absorption of light from the applied field by the atom can be regarded as interference between the applied light and the

light emitted by the atoms with a positive *v* component. In a similar manner, the light from atoms with negative *v* components will be in phase with the applied light field, which is interpreted as stimulated emission of light from the atoms.

When working with ensembles of atoms with different absorption frequencies, it is often convenient to consider the time evolution of the system in a frame that rotates with the optical frequency of the laser light. This means that atoms in a superposition state having absorption frequencies higher than that of the laser light will acquire positive phases (corresponding to clockwise rotation around the *w-axis*) and atoms absorbing at lower frequencies will acquire negative phases (corresponding to counter-clockwise rotation around the *w-axis*).

3. Rare-earth-ion-doped inorganic crystals

Elements with atomic numbers between 57 (lanthanum) and 70 (ytterbium) are called rare-earth (or lanthanide) elements. In these elements, the 4f shell of electrons is partially filled, containing one electron in the case of cerium (atomic number 58) and 13 in the case of ytterbium. The work presented in this thesis has been done using triply charged ions of some rare-earth elements, doped into inorganic crystals. In these ions, the 6s electrons and one 4f or 5d electron have been removed. The optical transitions in the ions involve the 4f electrons. These electrons are shielded from the environment by the outer-lying 5s and 5p electrons. This means that, due to the weak interaction with the environment, the ions retain many of the optical properties of free ions, even when doped into solid state hosts. When cooled to cryogenic temperatures (~4 K), rare-earth-ions doped into inorganic crystals have properties making them suitable for studying the coherent interaction between light and atoms in a way that is normally only possible using free atoms or ions. All the work described in this thesis has been performed on crystals at cryogenic temperatures. A thorough theoretical explanation of the optical properties of rare-earth-ion-doped crystals is beyond the scope of this thesis, but a short description of this type of material follows below. Excellent review articles on the optical properties of rare-earth-ion-doped crystals can be found in References 8-11. The investigations reported in this thesis have involved the elements europium (Eu), praseodymium (Pr) and thulium (Tm), see Figure 4.

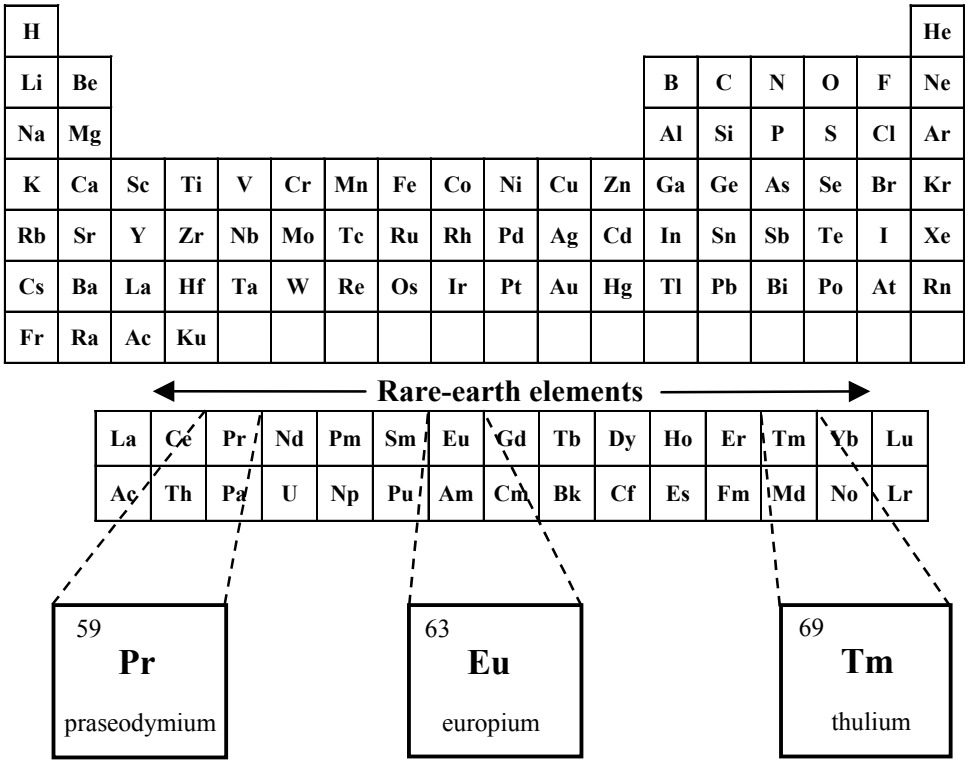

Figure 4. Periodic table where the rare-earth elements are shown. The elements that have been used in the investigations reported in this thesis have been magnified.

3.1. Homogeneous broadening

The most peculiar optical property of the rare-earth ions is their narrow homogeneous line widths of optical transitions involving the 4f electrons. The homogeneous line width is a measure of the width of the frequency interval in which each ion can absorb light. Homogeneous line widths, Γ_h, as small as 122 Hz have been reported for europium ions doped into Y_2SiO_5.[12] Recently, an even lower value of 50 Hz has been reported for $Er:Y_2SiO_5$ placed in a magnetic field of 7 T.[13] The homogeneous line width is directly connected to the optical phase memory, T_2, of the ions:

$$\Gamma_h = \frac{1}{\pi T_2}. \qquad (3.1)$$

Due to the weak coupling to the environment, and the absence of thermal phonons at cryogenic temperatures, the value of the phase memory can often approach the limit set by the lifetime of the excited state. However, for many combinations of dopant ions and hosts, other dynamic processes may contribute

significantly to reducing the phase memory. Fluctuating nuclear and electron spins of the atoms in the crystal host will shorten the phase memory of the ions. It is desirable to have a host material where the field variations due to flips of nuclear spins are small.[14] Yttrium oxides are good candidates because oxygen has zero spin and yttrium has a low magnetic moment. Lattice phonons can also reduce the phase memory, but at liquid helium temperatures the number of phonons with sufficient energy is often very low. However, at higher temperatures the contribution from phonons to the homogeneous broadening is often the dominating process. The homogeneous line width is also affected by interactions between the dopant ions themselves due to excitation or relaxation of the dopant ions in the crystal. This process is called instantaneous spectral diffusion, and has been studied extensively in rare-earth-ion-doped crystals, see e.g. References 15-18. Normally, instantaneous spectral diffusion has been considered a problem to be avoided but, as will be shown in Chapter 6 (Papers IV and V), it can, if utilised in a controlled way, also be used for quantum information processing in the crystals. The narrow homogeneous line widths of the ions have made it possible to use rare-earth-ion-doped crystals as frequency references when stabilising lasers to remarkable precision.[19,20]

3.2. Inhomogeneous broadening

Besides their narrow homogeneous line widths, rare-earth-ion-doped crystals also have inhomogeneous line widths that often are spectacularly narrow for solid state materials. The inhomogeneous broadening is the total frequency interval in which the ions can collectively absorb light. Another example of a system with inhomogeneous broadening is a gas experiencing Doppler broadening due to the spread in velocities of the different absorbers in the gas. Because of this and other similarities between the optical properties of gases and the rare-earth-ion-doped crystals, the latter have sometimes been referred to as “frozen gases”, see Figure 5. Whereas dynamic processes (to the first order) determine the homogeneous line widths of the ions, the inhomogeneous broadening is mainly caused by the static properties of the environment. Inhomogeneous broadening is mainly caused by strain in the crystal, but other effects can also contribute.[21] The strain is different in different parts of the crystal, causing different ions to shift their frequency by different amounts depending on their specific surroundings in the crystal. The strain can originate from the solidification of the crystal, but can also be caused by chemical impurities or other defects in the crystal lattice. For rare-earth ions doped into glass, the inhomogeneous broadening is normally much greater than that for crystals, due to the large variations in the unstructured host material. Typical inhomogeneous line widths for rare-earth-ion-doped crystals range from hundreds of MHz to hundreds of GHz. The inhomogeneous line width often increases with increasing doping due to the defects in the crystal lattice that the dopant ions themselves represent.[22] Because of the static nature of the inhomogeneous broadening it is, to the first order independent of temperature.

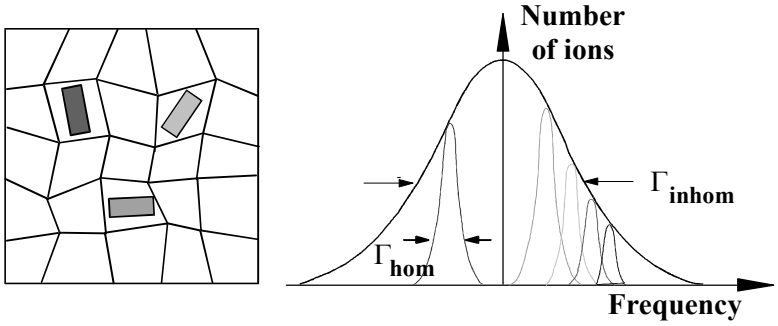

Figure 5. The different surroundings of the ions in the crystal host (left) shifts the absorption frequencies of the ions and creates an inhomogeneously broadened absorption line (right). Figure adopted from Reference 9.

3.3. Hyperfine levels

Ions doped into crystals experience an electrostatic crystal field due to the configuration of the charged ions constituting the crystal. The symmetry of the electric potential of this crystal field is important regarding its effect on the energy levels of the ions. Calculations of the crystal field in a crystal involve group theoretical considerations based on the symmetry of the crystal lattice. The interaction between the ions and the crystal field often splits energy levels that would be degenerate for free ions. For dopant ions with nuclear spin greater than ½, the electronic ground state of the ions is often split into hyperfine levels due to quadrupole interactions (second order hyperfine interaction) with the crystal field. The splitting is often in the range of a few MHz up to a few GHz.[8] The hyperfine levels are doubly degenerate, but the degenerate levels can be split into two if an external magnetic field is applied. This technique was explored in this work (Papers II and III). This splitting is particularly interesting in Paper II since thulium (Tm), with a nuclear spin of ½, has no zero field splitting of the ground state. By applying a magnetic field, the degeneracy between the two sublevels of the ground state was removed and the relaxation time between the two (Zeeman type) hyperfine levels was studied. After the acceptance of Paper II for publication, R. M. Macfarlane reported in a review paper on an experiment regarding the splitting of the ground state of Tm in YAG by the application of a magnetic field.[11]

In Figure 6, the results of a spectral hole burning experiment in Tm:YAG at applied magnetic fields of various strengths can be seen. In the experiment, an external cavity diode laser operated at 793 nm was used to burn a spectral hole, i.e. to remove the ions absorbing at a particular frequency, in the inhomogeneous absorption line of the Tm ions. Using the electro-optical crystal placed in the cavity of the laser,[23] the frequency of the light was chirped over 400 MHz around

the spectral hole and the transmitted signal was monitored. Each trace in Figure 6 represents such a signal for a specific value of the applied magnetic field. The increased transmission that can be seen at the centre frequency is the spectral hole, and the structures appearing symmetrically around the centre are due to the splitting of both the ground and excited states into two hyperfine levels. The structure with increased transmission (side holes) arise from hole burning from one of the ground state levels to one of the excited state levels, followed by probing from the same ground state level to the other excited level. The absence of population in the ground state will in this case lead to an increase in transmission, even when probed to a different excited state. The structures with decreased transmission (anti-holes) appear when the ions are probed from a different ground state level from the one used for the hole burning. In this case, the hole burning will result in an increased population in the ground state level with which the probe interacts, resulting in a decrease of the transmitted signal. From the positions of the side holes and the anti-holes it is thus possible to draw conclusions about the frequency of the splitting in the ground and excited states. In the experiment shown in Figure 6, the splitting in the ground state was approximately 80 MHz/T and in the excited state approximately 20 MHz/T. It should be noted that these results are only valid for the specific geometry used in the experiment, and that a different orientation of the magnetic field relative to the crystal would give other values of the splitting.

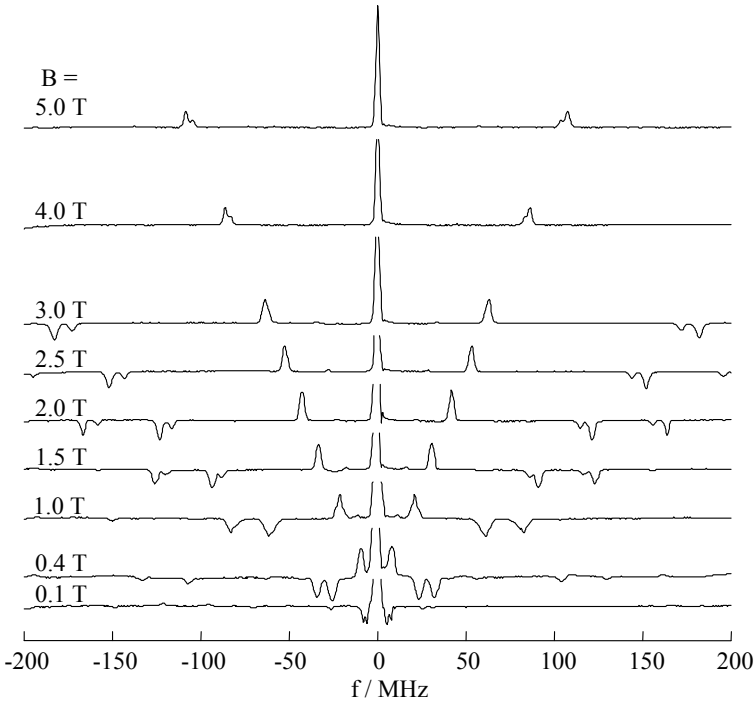

Figure 6. Spectral hole burning in Tm:YAG in external magnetic fields of various strengths. Each trace corresponds to a transmission measurement at a specific magnetic field strength. The probe pulse was scanned over 400 MHz during read-out. The transmission peak in the centre of the traces is the spectral hole and the structures appearing symmetrically around this peak are due to the magnetic field dependent splitting of the ground and excited states of the thulium ions.

4. Photon echoes

Photon echoes are the optical analogue of the spin echoes that were first studied by E. L. Hahn in 1950.[24] The first photon echo experiments were performed using a ruby crystal and a Q-switched laser.[25,26] The resemblance between spin echoes in nuclear magnetic resonance (NMR) and the optical photon echoes has been a source of inspiration, both in the development of photon echo theory, but also in proposals for a variety of applications where the photon echo process can be used. The complexity of the pulse sequences used in NMR experiments is far greater than those demonstrated at optical frequencies. This is mainly due to the fact that the applied pulses must normally have very well characterised phase and frequency contents, which is non-trivial to realise in practise in the optical domain. However, the use of ultra-stable lasers has recently made it possible to apply complicated pulse sequences, resembling those used in NMR, in photon echo experiments.[27-29] In this chapter, a description of the photon echo process will be given, followed by a few examples of the many proposed applications based on photon echoes and rare-earth-ion-doped crystals. The photon echo process was used in different ways in this work (Papers I, II and III).

4.1. The photon echo process

The photon echo process can be explained using the theory described in Chapter 2 when several optical pulses are applied to a collection of atoms with a long coherence time and inhomogeneously broadened absorption lines (such as the rare-earth ions doped into crystals described in Chapter 3). Other descriptions of the two- and three-pulse photon echo processes can be found in References 30-33.

In Figure 7, the pulse sequence in a two-pulse photon echo experiment can be seen. The aim of this section is to explain the action of each of the applied pulses and thereby explain the appearance of the photon echo. The ions will be assumed to constitute two-level systems. In many applications, several energy levels of the ions are utilised, but a model based on two levels coupled with a light field is still useful, and effects due to the other energy levels can often be considered by small modifications of this model.

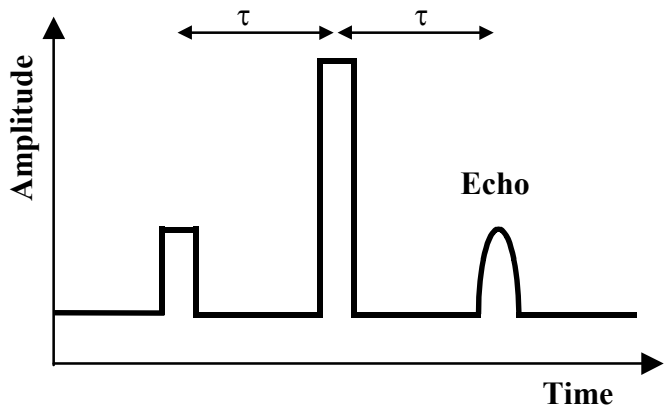

Figure 7. Pulse sequence for a two-pulse photon echo experiment, where two applied pulses give rise to a third pulse, the echo, that is emitted by the material.

Before the first pulse, all the ions are assumed to be in their ground states. This simplifies the discussion, but the important factor for obtaining an output signal is actually that there exists a population difference between the ground and excited states. The effect of the first pulse is to put the ions in a superposition of the ground and excited states. To simplify the discussion, the ions will be assumed to be in an equal superposition of the two states (i.e. the pulse is assumed to be a $\pi/2$ pulse, see Section 2.2). The probability of finding the ions in the excited state will vary depending on the detuning between the absorption frequency of the ions and the carrier frequency of the optical pulse, as described in Chapter 2. For a quantitative analysis of the efficiency of the photon echo process this detuning must be taken into account. However, the aim of this section is merely to explain the existence of the echo, and to simplify the explanation, this effect will be disregarded. This means that after the first pulse, all the ions are assumed to have Bloch vectors pointing along the *v*-axis in the Bloch sphere. The ions are then left to evolve freely. This means that the state of the ions will acquire a phase at a rate which depends on their absorption frequency. With the carrier frequency of the laser as the reference, this means that ions with an absorption frequency slightly above the frequency of the laser will acquire a positive phase proportional to the detuning and the ions absorbing at lower frequencies will attain a negative phase in the corresponding way, as described in Chapter 2. The result of this is that the Bloch vectors will spread out in the *uv*-plane of the Bloch sphere. When the second pulse is applied, the state of the ions will again be rotated around a pseudo-vector pointing along the *u*-axis. If this pulse is assumed to be a π pulse, the effect of the pulse will be that all ions will still be found in the *uv*-plane, but with a sign change of the *v* component, see Figure 8. The ions are now again left to evolve freely, and they will acquire different phases compared with the laser frequency depending on their transition frequency. At a time after the second pulse equal to the time between the first two pulses, the Bloch vectors for all the

ions will be aligned along the negative direction of the *v*-axis. This means that the states of all the ions will oscillate in phase at this moment in time. Since each ion in a superposition has a dipole moment associated with it (see Chapter 2), this means that the dipoles associated with all the ions will oscillate in phase and thus add up coherently. This will create a macroscopic dipole moment, which will lead to a coherent burst of light, the photon echo. As time progresses, the states of the different ions will again acquire different phases, which means that the dipoles associated with different ions will no longer add up, and the macroscopic dipole moment will therefore vanish.

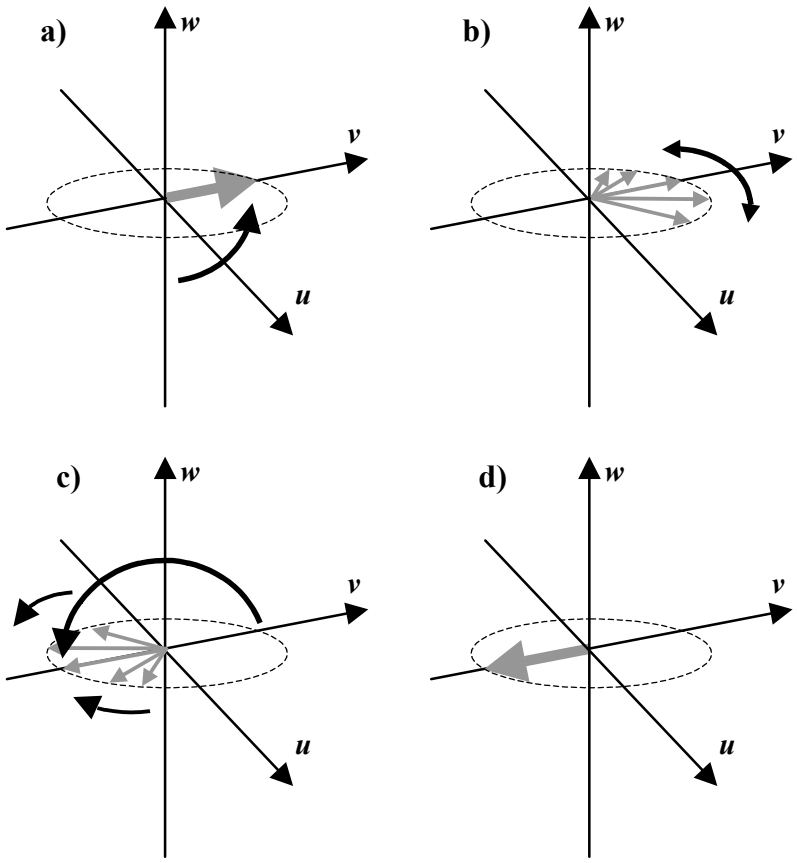

Figure 8. Bloch vector diagram for the two-pulse photon echo process. a) The first pulse transfers the atoms from their ground state to an equal superposition between ground and excited states. b) During the time between the two pulses, the atoms evolve freely. Depending on their absorption frequency, they acquire different phases and therefore spread out along the equator of the Bloch sphere. c) A π pulse reverses the sign of the v component of the Bloch vector of each atom. The atoms are the again left to free evolution. d) After a time corresponding to the time between the first two pulses, all the Bloch vectors become aligned along the negative v-axis resulting in a macroscopic dipole moment and the emission of a photon echo.

Another type of photon echo is the three-pulse photon echo, see Figure 9. In this case, the second pulse in the description above is divided into two pulses separated in time. Whereas the second pulse in the two-pulse echo sequence was assumed to be a π pulse, the optimal choice of pulse areas in the three-pulse echo process is for all three pulses to be π/2 pulses. In this case, the action of the second pulse is to create a frequency-dependent modulation of the population of ions in the ground and excited states. This can be accomplished since the second pulse will rotate the state of the ions one quarter of a cycle around the *u*-axis in the Bloch sphere. This means that ions with a positive *v* component will be transferred towards the excited state, whereas ions with a negative *v* component will end up closer to the ground state. This will create a periodic modulation of the population in the ground and excited states as a function of transition frequency. This modulation of the population is often referred to as a population grating. Under the action of the third pulse, ions in their ground state will be transferred to a superposition along the positive *v*-axis, whereas the ions residing in the excited state will be transferred to a superposition along the negative *v*-axis. An examination of the phase accumulation of the different ions shows that after a time corresponding to the time between the first two pulses, all the phases of the ions will be the same and an echo will be produced.

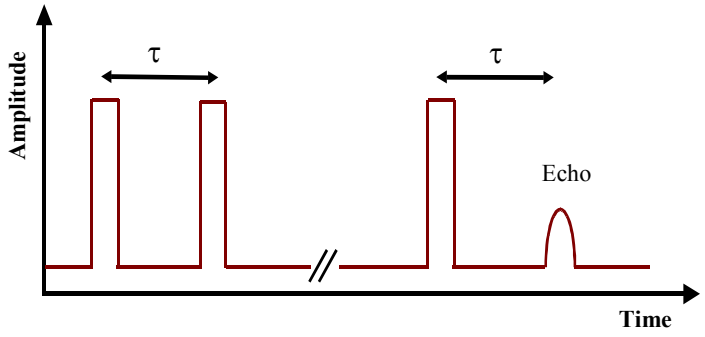

Figure 9. Pulse sequence for the three-pulse photon echo process, where coherent interaction between three applied pulses and the material gives rise to a photon echo.

A careful analysis of the photon echo process shows that the intensity of the echo signal, I_e, in the three-pulse echo process can be written as[34]:

$$I_e \propto \sin^2(\theta_1)\sin^2(\theta_2)\sin^2(\theta_3), \qquad (4.1)$$

where $\theta_{1\text{-}3}$ are the pulse areas of the three applied pulses. For pulses with small pulse areas and a fixed duration, the echo signal will be proportional to the product of the intensities of the three applied pulses. In the case of the two-pulse echo, the second pulse simply replaces the second and the third pulses in the equation, meaning that θ_3 is replaced by θ_2 in Equation 4.1 above.

Even if the upper state population has decayed between the second and third pulses in the three-pulse echo sequence, spectral features can still be stored in the ground state population and give rise to an echo after the third pulse.[35,36] This population storage can take place; either by involving a third meta-stable electronic state or in the different hyperfine levels of the ground state, e.g. in europium-doped crystals.[37]

It is possible to replace the two first pulses in the three-pulse photon echo process by direct periodic hole burning in the frequency domain.[38] This experiment is, in my opinion, a beautiful demonstration of the relation between the time and the frequency domain and gives a strong indication that the picture of the photon echo presented above is correct.

In both the two- and the three-pulse echoes, the echo will be emitted only in one direction. This direction is determined by the phase matching condition, in the same way as for other non-linear optical processes.

4.2. Applications

The photon echo process can be used in spectroscopy to reveal the homogeneous line width of an absorber even if it is hidden under a broad inhomogeneous profile. The use of photon echoes with the purpose of obtaining spectroscopic information has been applied to a vast number of physical systems, see e.g. References 8 and 9. This section will, however, be focused on applications in the field of information science. The use of photon echoes in such applications was first discussed during the late 1970s and early 1980s.[39,40] At first, rather simple applications such as time reversal and simple all-optical memories based on three pulse echoes were considered, but since then a large number of applications in a variety of different fields have been proposed. In this section, developments in the field of photon-echo-based memories will be briefly reviewed, some of the many proposals for signal processing using photon echo techniques will be explained, and in the last part, a more detailed description of optical pulse compression using photon echoes will be given (this is also the topic of Paper I).

4.2.1. Memories

The possibility of using spin echoes in NMR for the construction of a data storage device was discussed and experimentally investigated in the 1950s.[41] A photon-echo-based memory device was proposed by T. W. Mossberg in 1982.[40] The photon echo memory has been argued to have the potential of commercialisation due to its capability for storage of large amounts of data in a single spatial location, its capability to store pulses with short duration and thus handle high data rates and the possibility for long storage times without the need for refreshing of the stored data.

The simplest case of data storage using photon echoes is the three-pulse echo technique described above. If the second pulse in this process is replaced by a sequence of (weaker) pulses, a replica of these pulses will be sent out after the third pulse, see Figure 10. The theoretical limit for the amount of data that can be

stored in a single spatial location is given by the ratio between the inhomogeneous and the homogeneous line widths, which for some combinations of rare-earth dopant ions and host crystals can be as high as 10^8.[13] Several attempts have been made to calculate the maximal storage density for a photon-echo-based storage device, and storage densities of up to Tb/cm^2 have been predicted.[34,42] In a practical application, many parameters must be considered, such as the speed at which data are written and read from the memory, the requirements on latency and the optical power needed in the device. A problem with this approach is that high data rates are often desirable in data storage applications. This means that short pulses have to be used in the photon echo process. Short pulses normally mean that a high peak power is needed to achieve the desired pulse area of $\pi/2$ for the first and the third pulses in the photon echo process, which puts heavy demands on the laser source.

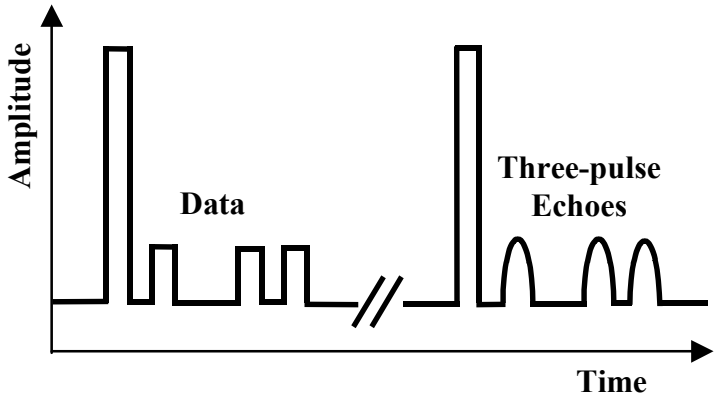

Figure 10. Optical pulse sequence used in data storage using photon echoes. The process is similar to the three-pulse photon echo process, but the third pulse is replaced by a number of data pulses.

A technique where chirped pulses are used to store the data is the so-called swept-carrier technique.[43] This technique can be viewed as a hybrid between storage in the time and the frequency domain. In this approach the first pulse in the three-pulse echo sequence is replaced by a longer frequency-chirped pulse and the carrier frequency of the light is chirped in the same way also during the data stream. When a third chirped pulse (the read-out pulse) is sent into the crystal, a replica of the data will be sent out at each frequency after a time corresponding to the time difference between the interactions of the first pulse and the data pulses at that frequency. This can be seen in Equation 4.3 if the first and the third are set to be constant over all frequencies (corresponding to frequency chirp over all relevant frequencies). The result is then a Fourier transform of the frequency content of the data stream, i.e. a replica of the temporal shape of the data.

In the swept-carrier approach, the first pulse and the data stream can be partially overlapped in time, i.e. the first pulse does not have to end before the

data stream is switched on.[43] An advantage of using the swept-carrier approach and overlapping the reference beam and the data stream in time is that all the data do not have to be written within the phase memory time of the photon echo material. Using a diode laser of the same type as the one used in the experiment described in Paper I, 4 kbit of data were stored at a single spatial location.[44]

Applying a magnetic field can increase the storage time in the hyperfine levels of the ground state (see Chapter 3). This technique was used in the work described in Papers II and III, and could also be used in long-time data storage applications. Paper II presents a simple data storage experiment where the swept-carrier technique was used to show the feasibility of long-time data storage in a Tm:YAG crystal when an external magnetic field was applied, see Figure 11.

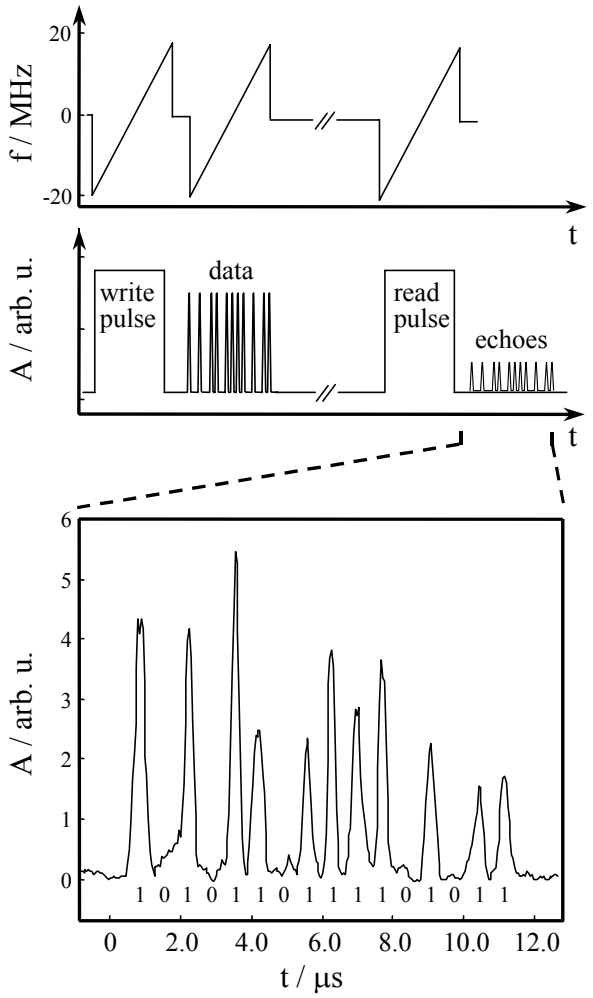

Figure 11. Storage of 16 bits of data in a Tm:YAG crystal for 200 ms. In the upper part, the amplitude and frequency of the applied pulses is shown, and in the lower part an experimental trace of the resulting echoes is shown.

4.2.2. Optical signal processing

A large number of applications of the photon echo process in all optical signal processing have been considered. In this thesis only a few will be briefly reviewed. The greatest advantage of photon echo based devices, compared with electronic devices, is the many degrees of freedom that can be utilised in their implementation. These include the ability to process information on the basis of the temporal information, the frequency content, the spatial structure (in three dimensions) or the angle of incidence of the light pulses in the photon echo material. Because of the relatively high technical complexity of a photon-echo-based device, applications in which as many of these degrees of freedom as possible are utilised will, in my opinion, have the greatest potential to compete with conventional electronics. Because of the demands placed on the equipment (cryostats, frequency-stabilised lasers, etc.) used in connection with photon echo experiments, applications where these demands do not constitute a problem seem the most promising ones.

The basis for most applications based on the photon echo process is the inherent ability to perform correlations and convolutions. For excitation pulses that are far from saturating the transitions (pulse areas significantly below $\pi/2$), the output field in a three-pulse echo process can be written as:

$$E_{echo}(t) \propto E_1(t) \otimes \left(E_2(t) * E_3(t)\right), \tag{4.2}$$

where $\otimes$ denotes a correlation and * a convolution operator. The relation can also be expressed in the frequency domain:

$$E_{echo}(t) \propto \int_{-\infty}^{\infty} E_1(\omega)^* \cdot E_2(\omega) \cdot E_3(\omega) \cdot e^{-i\omega t} d\omega \,. \tag{4.3}$$

Using this relation either in the time or in the frequency domain, various types of signal processing can be implemented. As an example, it has been proposed that the photon echo process could be used for spectral analysis of radio frequency signals.[45] Further, it has been proposed that the photon echo process could be used to impose a variable time delay on an optical signal.[46] This could be used for so-called true time delay generation in radar applications in connection with phased array antennas. A number of experimental tests on the true time delay application have been performed, see e.g. References 47-49.

Several applications of the photon echo process in the field of optical communication have been considered. Spatial routing of optical beams into directions that depend on the temporal structure of the beams has been proposed.[50] The proposal was followed by a proof of principle experimental demonstration.[51] A similar idea is that optical header information can be extracted from a stream of data by programming the headers into the photon echo material at different angles, before the data stream is sent to the material.[52] The existence of the pre-programmed headers in the data would result in photon echoes being sent out in directions characteristic of the different headers. A demonstration of optical

header recognition was later performed in the telecommunications window at 1536 nm, the wavelength at which most optical fibre communication takes place.[53]

4.2.3. Pulse compression using photon echoes

Temporal compression of optical pulses using the photon echo process was first proposed and studied experimentally in a gas sample by Mossberg and co-workers.[54,55] The same approach was later studied using a rare-earth-ion-doped crystal as the active medium.[56] In another study, an analogous technique aimed more directly at altering the bit rate of a data stream was utilised.[57] Improved pulse compression using optical pulses from an external cavity diode laser is the topic of Paper I.

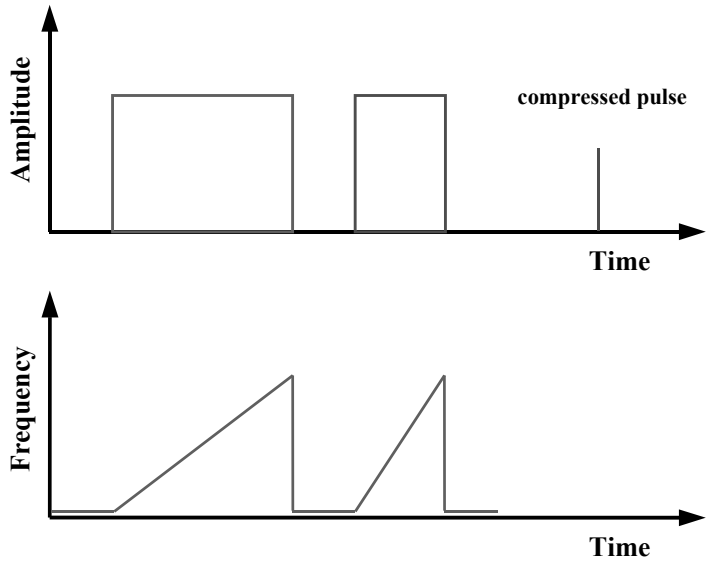

Figure 12. Pulse compression can be performed in a two-pulse photon echo process by applying appropriate frequency chirps to the optical pulses. If the second of the two excitation pulses is chirped at a rate that is twice that of the first one, all the atoms affected by the two pulses will rephase at the same time, sending out a short burst of light. The duration of this pulse is proportional to the inverse of the bandwidth covered by the chirped pulses.

In Figure 12, the amplitudes and frequency chirps needed for compression in a two-pulse echo experiment are shown. The chirp rate of the second pulse should be exactly twice that of the first pulse. The compression process can be understood in an intuitive way. In the two-pulse photon echo, the ions emit a pulse at a time after the second interaction that is exactly the same as the time between the first and the second interaction. Using the chirp rates depicted in Figure 12, the interaction with the ions absorbing light at different optical frequencies takes place at different times, but the chirps are tailored so that all ions will emit their

echo at the same time. The initial duration of the chirped optical pulses to be compressed in the process is limited by T_2 of the ions in the crystal, since the ions have to keep their phase memory from the first interaction until the compressed pulse is emitted as an echo. The duration of the compressed pulse is, as mentioned above, related to the bandwidth of the chirped optical pulses, but is ultimately limited by the inhomogeneous broadening of the optical transition used for the compression process.

The following derivation of the shape of the compressed pulse is similar to that given in a recent paper where the possibility of using chirped pulses in the photon echo process for spectrum analysis of signals is investigated.[45] The two chirped input fields used in the compression sequence can be described as:

$$E_j(t) = g_j(t) A_j e^{-i\omega(t-t_j)} e^{-iK_j(t-t_j)^2} \quad ; \mathrm{j} = 1,2 \quad ; \tag{4.4}$$

where K is the chirp rate of the pulse and ω is the carrier frequency of the light. The functions $g_j(t)$ describe the temporal shape of the pulses and can be used to describe e.g. a bit pattern for the first pulse. To make the calculations simpler, we assume that the arrival of the first pulse at the medium is centred around time $t=-t_1$, and the second at $t=0$, and we therefore expect the echo at $t=+t_1$. In the time domain the echo pulse is calculated using Equation 4.2 above, but with only two different input fields:

$$E_{echo}(t) \propto E_1(t) \otimes E_2(t) * E_2(t) \,. \tag{4.5}$$

We start with the second field convoluted with itself and assume that the chirp of this pulse has an infinite extent in time, i.e. we assume that $g_2(t)=1$ for all times:

$$\begin{aligned} E_2(t) * E_2(t) &\propto A_2^2 \int_{-\infty}^{\infty} e^{-i\omega\tau} e^{-iK_2\tau^2} e^{-i\omega(t-\tau)} e^{-iK_2(t-\tau)^2} d\tau = \\ &= A_2^2 e^{-i\omega t} e^{-iK_2 t^2} \int_{-\infty}^{\infty} e^{-i2K_2\tau^2} e^{i2K_2 t\tau} d\tau = \\ &= \sqrt{\frac{\pi}{2iK_2}} A_2^2 e^{-i\omega t} e^{-i(K_2/2)t^2} \,. \end{aligned} \tag{4.6}$$

The echo is now given by:

$$E_{echo}(t) \propto E_1(t) \otimes E_2(t) * E_2(t) \propto$$
$$\propto A_1 A_2^2 \sqrt{\frac{\pi}{2iK_2}} \int_{-\infty}^{\infty} g_1(\tau) e^{i\omega(\tau+t_1)} e^{iK_1(\tau+t_1)^2} e^{-i\omega(t+\tau)} e^{-i(K_2/2)(t+\tau)^2} d\tau = \qquad (4.7)$$
$$= A_1 A_2^2 \sqrt{\frac{\pi}{2iK_2}} e^{-i\omega(t-t_1)} e^{iK_1 t_1^2} e^{-i(K_2/2)t^2} \int_{-\infty}^{\infty} g_1(\tau) e^{i(K_1-K_2/2)\tau^2} e^{i2K_1\tau t_1} e^{-iK_2\tau t} d\tau$$

If we now explicitly consider the compression experiment described above, and assume that the chirp rate of the second pulse is twice that of the first, the following echo field is obtained:

$$E_{echo}(t) \propto A_1 A_2^2 e^{-i\omega(t-t_1)} e^{-iK_1(t^2-t_1^2)} \int_{-\infty}^{\infty} g_1(\tau) e^{-i2K_1(t-t_1)\tau} d\tau \,. \qquad (4.8)$$

We see that the echo pulse appears at time t_1 as expected. The integral appearing in Equation 4.8 is a Fourier integral, making the echo shape proportional to the Fourier transform of the temporal shape of the first pulse, with the frequency scale given by $2K_1t$. As expected, the resulting echo will therefore be shorter if the first pulse covers a wider frequency interval within its duration.

Pulse compression using photon echoes has been proposed for use in connection with data transmission in optical fibres. The idea would be to compress the data streams before sending them through the fibre, thereby enabling time multiplexing of different data streams. This would allow better utilisation of the available bandwidth of the optical fibre. At the receiving end of the fibre, the reverse process (again using photon echoes) could be employed to decompress the data. This procedure has an advantage over merely increasing the bit rate of the data stream in that it is all-optical and does not require electronics fast enough to detect the compressed data. A problem with this approach, however, is that the compressed signal is normally much weaker than the original data. In order to first compress and then decompress the data all-optically, it therefore appears to be necessary to amplify the signal before the decompression stage. The use of fibre amplifiers for amplification and regeneration of photon echoes has been investigated for the case of $Pr:Y_2SiO_5$.[58,59] The alternative to the time multiplexing technique described above is the wavelength division multiplexing (WDM) technique, where information is transmitted at lower data rates, but in many wavelength channels simultaneously. The WDM technique has been commercialised and is being implemented in optical communications networks around the world.

Photon-echo-based pulse compression is a simple demonstration of the use of relatively high bandwidth programming of a photon echo material and indicates that more complicated optical programming at high bandwidths for other applications is feasible.

Further experiments on pulse compression using coherent transients have recently been reported and connections to general pulse shaping have been made.[60] In Reference 60, temporally overlapped pulses with different chirp rates

were used for compression, in a way similar to the swept-carrier data storage technique described above.

5. Delayed single-photon self-interference

In this chapter, the experiment that is reported in Paper III will be elaborated upon. Firstly, a few comments on quantum optics will be given. Then the idea behind the delayed single-photon self-interference experiment, reported in Paper III, will be described. In the next section, some comments on the experimental realisation and the work preceding the final experiment are given. Finally, this chapter ends with some general comments on the experiment and the connection between the delayed single-photon self-interference experiment and a few other proposed and experimentally realised experiments in the field of quantum optics.

For a detailed description of the interaction between light and atoms, the theory in Chapters 2 and 4 must be modified to take into account the fact that an electromagnetic field can only consist of discrete entities of energy, see e.g. Reference 4. The use of this full theory for the interaction between the quantised electromagnetic field and atoms is beyond the scope of this thesis. However, many quantum optical effects can still be understood intuitively.

5.1. Quantum optics

The wave-particle duality of light has been a central issue in the development of quantum mechanics. Young's double slit experiment has been used as a Gedanken experiment to illustrate the possibility of single quantum objects (e.g. electrons or photons) interfering with themselves. In this experiment, a single quantum object can travel two possible paths to a detector. If measurements are made, the object will (as expected) be found in one of these paths. However, if no measurements are made, an interference pattern will arise, indicating that the object actually travelled along both paths simultaneously. This type of mysterious self-interference for single quantum objects was described by Richard Feynman as "the only mystery in quantum mechanics".[61] The development of quantum optics in its modern form started in 1927 when Dirac proposed that each mode of the electromagnetic field could be described using a quantised harmonic oscillator.[62] The rapid development in experimental quantum optics during recent decades has

made it possible to experimentally test the theories of quantum mechanics and, in many cases, Gedanken experiments proposed in the early days of the development of quantum mechanics have been realised with almost no modifications.

Many experiments in quantum optics investigate effects due to single photons. However, creating true single photon states is a difficult experimental task. An alternative way of performing the experiments is to use highly attenuated laser pulses. The number of photons in a laser pulse has an uncertainty and the photon number can be approximated by a Poisson distribution, see Figure 13. This means that "identical" pulses from a laser will, when measured, not be found to contain the same number of photons. If the laser pulses are attenuated so as to contain very few photons, the contributions to the signal from pulses containing different numbers of photons can be calculated using the Poisson distribution and effects due to single photons can thereby be deduced. This was utilised when analysing the results presented in Paper III.

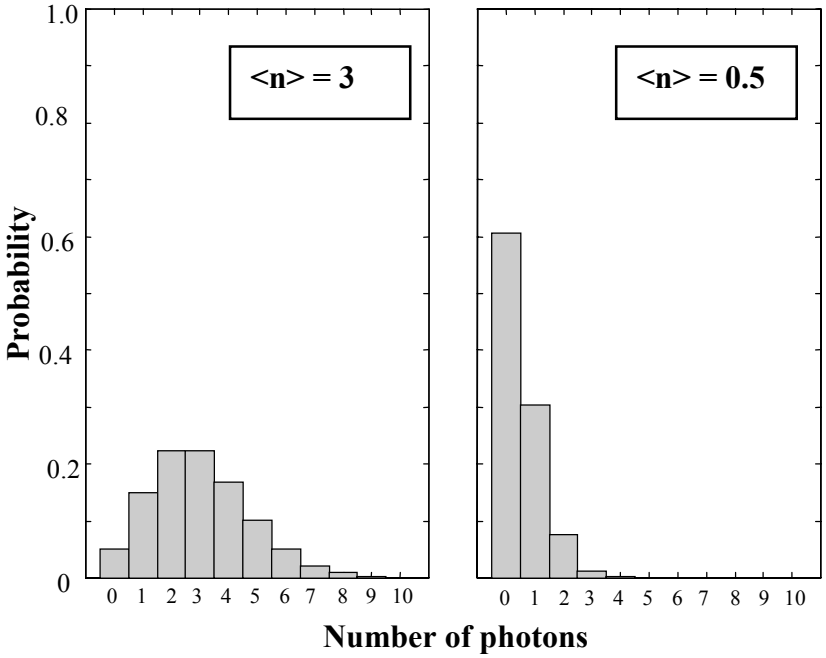

Figure 13. The probability distribution for finding different numbers of photons in coherent states containing, on average, 3 photons (left) and 0.5 photons (right).

5.2. Echoes with single photons

The possibility of a single photon acting twice on a photon echo material, thereby producing a population grating, was first suggested by Kessel and Moiseev in 1993.[63] Their idea was that the first two pulses in the three-pulse photon echo experiment could consist of only one photon in a superposition state of the two

pulses. In the original proposal, this was to be accomplished by splitting the photon using a beamsplitter, delaying the path from one of the beamsplitter ports to the material and then overlapping the two paths at the photon echo material (see Figure 14). The delay between the two paths should be greater than the duration of the single photon wave packet, in order to separate the interaction into two events taking place at different times. After the accumulation of many interactions between single photons and the photon echo material, Kessel and Moiseev proposed that it would be possible to send in a strong light pulse and, after a time equal to the delay between the two arms of the interferometer, detect an echo. Detection of this echo would be an indication that each single photon had acted twice on the material, since two different photons would not produce a signal with this specific delay.

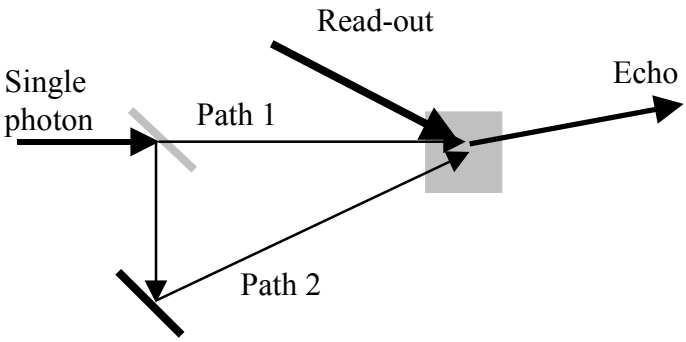

Figure 14. The interferometric set-up originally proposed for use in the delayed single-photon self-interference experiment. Single photons impinging on a beamsplitter have two paths along which they can travel to the photon echo material. The delay between the two paths is greater than the length of the photon wave packet. Since the wave packets from the two paths do not overlap in both time and space, interference in the overlap region can not be detected using a normal detector. However, when a photon echo material is used for detection, self-interference of the photons will take place and an interference pattern will be formed in the material.

Detailed calculations of the signal in the delayed single-photon self-interference experiment described above, involve the full theory of interaction between a non-stationary (multi-mode) quantised electromagnetic field and a collection of absorbers with inhomogeneous broadening, see e.g. References 63 and 64. Here, I will try to give an intuitive picture of the process since I believe that such a picture is very useful in gaining a better understanding of physics in general. However, quantum optics often leads to non-intuitive results, so one should be careful when drawing conclusions about the outcome of experiments based on the (incomplete) model.

Before any interaction between the photon and the material has taken place, all the absorbers are assumed to be in their ground state. After passing the beamsplitter, the photon is in a superposition of the two possible paths. When the light travelling along the shorter of the two paths has had time to interact with the material, this superposition is transferred into a superposition of a photon travelling along the other path and one excitation in the material. However, since the material consists of a large number of absorbers, the absorption process will not involve a specific absorber, but rather create a superposition of excited absorbers in the frequency interval covered by the single photon wave packet. During the delay between the two photon paths, this superposition of absorbers in the excited state will evolve freely, and the absorbers will accumulate different phases due to their different absorption frequencies (as in the normal three-pulse photon echo process). When the light travelling along the longer optical path interacts with the material, it will enhance the probability of ions at some frequencies to be in the excited state (due to constructive interference), and bring ions at other frequencies back to the ground state, depending on the phase of the wave function of the ions relative to that of the optical field. If the photon contained in the two pulses is absorbed by the ions in the crystal, the expectation value of the number of ions that can be found in their excited state is equal to one, but the probability is spread over a large number of ions. If several single photons are sent into the sample, a population grating will slowly build up, ion by ion, as for the normal three-pulse echo described in Chapter 4. Even if the ions have time to decay, there will still be a modulation in the ground state population, as long as the ions decay to a state different from their original ground state. As mentioned in Chapter 4, a population grating in one of the levels interacting with the field is sufficient to produce a photon echo signal.

The experiment is similar to Young's double slit experiment since the photon can travel along two possible paths that are overlapped at the photon echo material, which acts as a detector. The experiment is different from a normal interference experiment since wave packets travelling along the two possible paths never overlap temporally, i.e. they are never at the same place at the same time. Because of this peculiarity, the experiment has been denoted delayed single-photon self-interference. In fact, two different types of interference will take place in the photon echo material. The delay between the photon paths will create frequency-dependent modulation of the population in the material, and the angle between the two paths will create spatial modulation of the population.

5.3. Experimental considerations

5.3.1. Photon echo material

The initial part of the work on realising the delayed single-photon self-interference experiment was focused on trying to find a photon echo material that was well suited for the experiment. Calculations of the signal strength had shown that both rare-earth-ion-doped crystals and dye-doped organic films had the

potential to be the active medium in the experimental realisation of the experiment.[65] In the first stages of the work, dye-doped organic materials seemed to be the best choice. This was mainly due to the high oscillator strengths of the optical transitions in the dye molecules. A good candidate for the experiment seemed to be the dye aluminium phtalocyanine tetrasulphonate (APT) in organic films.[66] Hole burning experiments on an APT sample provided by the group of G. J. Small, were performed. In this case, APT was mixed into a film made of pHEMA. Homogeneous line widths of a few GHz were observed in the experiments.

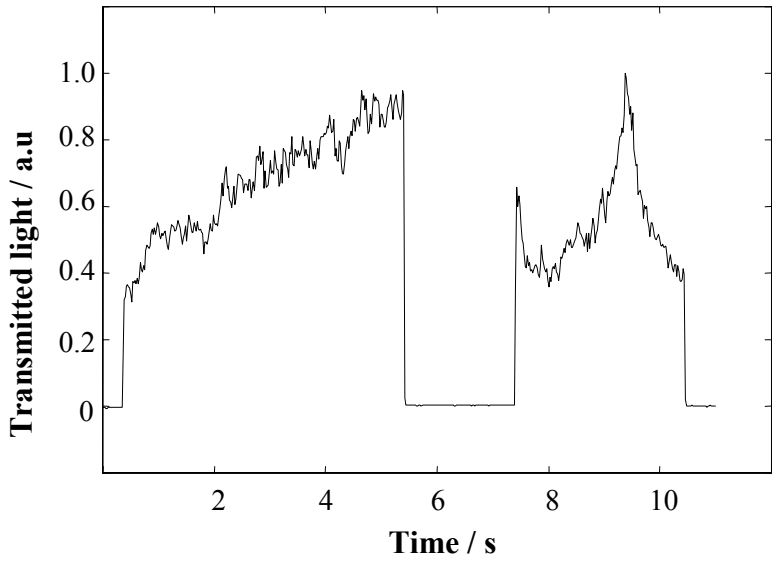

Figure 15. Spectral hole burning in APT in pHEMA using a ring dye laser. The figure shows the transmission of the pulses used for the hole burning. First a pulse with a fixed frequency was applied to the material. This pulse can be seen to saturate the optical transition (the transmission increases with time). Then a second pulse was applied and the frequency of the light is scanned 10 GHz around the frequency at which the spectral hole was burnt, and the spectral hole can be seen as a peak in the transmission. The width of the peak gives an indication of the homogeneous optical line width of the molecules in the material, in this case approximately 1 GHz.

A picosecond dye laser system was also installed and preliminary echo experiments were performed on octaethyl-porphyrin (OEP) in PMMA. However, the use of picosecond laser pulses and an interferometric set-up presents a major experimental challenge. For the frequency modulations produced by the individual photons to add up coherently, the path difference between the two arms of the interferometer must be kept stable to significantly less than an optical wavelength during the whole accumulation time. According to calculations, the accumulation time required to obtain a detectable echo signal is of the order of ten

minutes. At this stage of the work, it was realised that an interferometer with this stability was probably not necessary to realise the experiment. Instead, it was suggested that pulses carved out by a modulator from a continuous laser could be used.[67] In this way, the two photon paths in the original suggestion would be replaced by two pulses from the modulator. In this way, the pulses would travel the same path to the photon echo material, which means that no spatial modulation pattern will be created. If the separation between the pulses is chosen to be smaller than the coherence time of the laser, the light in the two pulses would have the same phase relation for all accumulated pulses. In fact, this condition replaces the requirement of stability of the interferometer in the original proposal. If the light in the pulses is attenuated so that the two pulses contain only a single photon, this photon would be in a superposition of being in the two pulses. This also means that this superposition can be transferred to the atoms in the materials, as in the original proposal, and that an echo signal can be created.

Using external modulators to create the pulse pairs meant that it was impossible for us to create pulses shorter than a few tens of nanoseconds. This placed constraints on the phase memory of the photon echo material that was to be used in the experiment, since the phase memory has to be considerably longer than the separation between the pulses in the pulse pairs for the photon echo process to be efficient. This ruled out the dye-doped organic materials that were tested in the early stages of the project, since their GHz-wide homogeneous line widths correspond to phase memory times of less than one nanosecond. We therefore turned our attention towards rare-earth-ion-doped crystals. At first, europium-doped crystals were considered, and the accumulation of pulse pairs containing, on average, less than 1000 photons in $Eu:Y_2SiO_5$ was seen to give detectable echo signals. The choice of europium-doped crystals was motivated by the long relaxation time between the hyperfine levels, up to several hours, that can be found in these crystals. Calculations showed that accumulations of up to hours would be necessary for a sufficiently strong population grating to build up. The total accumulation time that can be used in the experiment is ultimately limited by the storage time of the spectral modulation pattern in the material. Two difficulties were identified in these experiments. First, the long-time frequency stability of the ring dye laser was not good enough to perform reliable accumulations for several minutes. Second, the low oscillator strength of the optical transition for europium made it difficult to reach the single-photon level while keeping the accumulation time reasonable. The solution to the first problem will be described in the next section. To improve on the second point, crystals doped with other rare-earth elements were considered. The natural choice was crystals doped with praseodymium, since e.g. $Pr:Y_2SiO_5$ has an oscillator strength at least one order of magnitude greater than the corresponding europium doped crystal, and because praseodymium has three hyperfine levels in the ground state. However, the relaxation time between these levels is normally only around 100 s,[68] which would not give us a long enough accumulation time to obtain a detectable signal. However, when an external magnetic field was applied, the hyperfine level lifetime was observed to increase significantly (see Paper III). Subsequent experiments were thus performed using $Pr:Y_2SiO_5$ as the active material.

5.3.2. The light source

$Pr:Y_2SiO_5$ absorbs light at 606 nm, a wavelength that can conveniently be reached using dye lasers. The dye laser used in the experiment was a Coherent model 699-21 ring dye laser. When lasing in a single cavity mode, this laser has a short-time line width of around 1 MHz. Long-time frequency stability of the laser is obtained by locking to an external temperature-controlled reference cavity. This keeps the laser within a frequency interval of about 50 MHz on a timescale of about one hour.

The frequency separation between the fringes in the spectral population grating produced by the pulse pairs in the experiment is given by the inverse of the time between the pulses within the pairs. However, the exact location of the fringes, i.e. the phase of the modulation pattern in the frequency domain, will be determined by the relative phase of the light in the two pulses within each pair. For the spectral gratings from different pairs to add up constructively, it is therefore imperative that the relative phase between the pulses be the same for all the pairs to be accumulated. In other words, the laser used in the experiment must be phase stable, to a high degree, during the time separation between the pulses within the pairs. In a similar way, frequency drift of the laser during the accumulation sequence will also move the position of the spectral gratings, and therefore long-time frequency stability better than that set by the frequency difference between the fringes in the frequency domain is required of the laser. In the experiment reported in Paper III, a separation between the pulses in the pulse pairs of 175 ns was used. This corresponds to a fringe separation of 5.7 MHz. According to the above numbers, the short-time line width of the laser was adequate for the experiment, whereas the long-time stability had to be improved upon. This was accomplished by locking the frequency of the dye laser to a hyperfine transition in molecular iodine.[69] A saturation spectroscopy set-up, with two counterpropagating beams was used to obtain a Doppler-free spectrum of the hyperfine levels of the iodine molecules. One of the beams (the pump) was frequency modulated using two acousto-optic modulators placed in series. The other beam (the probe) was monitored with a photodiode, and the signal was extracted using a lock-in amplifier working at the modulation frequency of the pump beam. This resulted in hyperfine lines with dispersion-shaped curves. This signal could be used as an error signal that could be sent via an electrical integrator to the frequency control input of the laser. In this way, the long-time frequency stability of the laser was improved, and the frequency drift was found to be only a few MHz as long as the laser was locked to the same iodine line.

5.3.3. Optimising the echo signal

Because of the non-linear dependence of the echo signal on the intensities of the excitation pulses, correct focusing of the excitation pulses onto the crystal is of importance in obtaining an optimal echo signal. In theory, optimal focusing of the excitation pulses is achieved when the volume of the focus is so small that even if almost all the ions within the volume contribute to the signal, this signal is close to the detection limit of the experiment. The reason for this is that tighter focusing

means that the single photons in the pulse pairs will correspond to a higher intensity which, in the non-linear photon echo process, will result in a stronger signal. On the other hand, too tight focusing will mean that the number of ions within the volume exposed to the pulses will not be large enough to produce a detectable signal. The focal spot finally chosen for the experiment presented in Paper III, was significantly larger than the optimal choice according to the above. Several different focusing conditions were investigated experimentally, and although smaller focal spots gave improved signals for short accumulation times, the one used in the experiment was found to be best for the longer accumulation sequences (up to one hour). We believe that the reason for this is that small movements (vibrations) of the crystal on longer time scales will affect the signal more if a small volume is used. If this is the case, the signal in the experiment might be improved if a more stable mounting system for the crystal were to be constructed.

Another factor that could possibly have improved the signal in the experiment is the following; If a more phase-stable laser had been available for the experiment, this would have allowed the separation between the pulses within the pairs to be chosen more freely. Together with the ability to change the applied external magnetic field, which splits the hyperfine levels in both the ground and excited states, it might have been possible to find combinations of hyperfine level splittings and pulse separations rendering substantially larger signals than those observed in the experiment reported in Paper III. The reason for this is that when the excitation pulses (in the pairs and the read-out) are short enough to cover several hyperfine levels in the ground and/or in the excited state, photon echoes can be formed on many different optical transitions simultaneously. If the time between the pulses, and thus the periodicity of the frequency modulation, is chosen carefully, the contributions from most of these different transitions could be made to interfere constructively, thus rendering a larger echo signal. Resonances of this type have been explored in echo experiment using strong pulses to extract information on the splitting between the hyperfine levels.[70]

5.3.4. The detection system

To minimise the required accumulation time in the experiment, it is desirable to have a detector that can detect an echo signal containing as few photons as possible. This means that a detector with high quantum efficiency should be used. The detectors with the highest quantum efficiency, and that are normally used for detecting pulses containing few photons, are avalanche photodiodes. However, these detectors have a poor dynamic range and take a long time to recover after being saturated. This is a problem in the present experiment, since the strong read-out pulse that arrives just before the weak echo signal easily saturates the detector. In the experiment, a photomultiplier tube (PMT) was therefore used instead to detect the signal. PMTs have quantum efficiencies slightly lower than the best avalanche photodiodes, but have a much better dynamic range. Even when using a PMT as the detector, preventing the detector from being saturated by the strong read-out pulse was still a major issue. The read-out pulse used in the experiment contained of the order of a billion photons, and arrived at the detector only 175 ns

before the weak echo signal. Two acousto-optic modulators placed in series, giving an extinction of about $1{:}10^4$, were used as a gate in front of the detector. Electro-optic modulators were also considered, but due to the fact that the acousto-optic modulators are easier to handle, they were chosen for the experiment. Even if the read-out pulse does not saturate the photomultiplier tube, after-pulses and noise might prevent the detection of the weak signal.

5.3.5. Experimental results

In the experimental realisation of the experiment, accumulation times of up to one hour were used before the read-out pulse was applied and the echo signal was detected. The minimum number of photons per pulse pair used was 0.54 and resulted in the signal that can be seen in Figure 16. In this experiment, a total of $7{\cdot}10^9$ pulse pairs were accumulated before the signal was read out. For further details on the experiment, see Paper III.

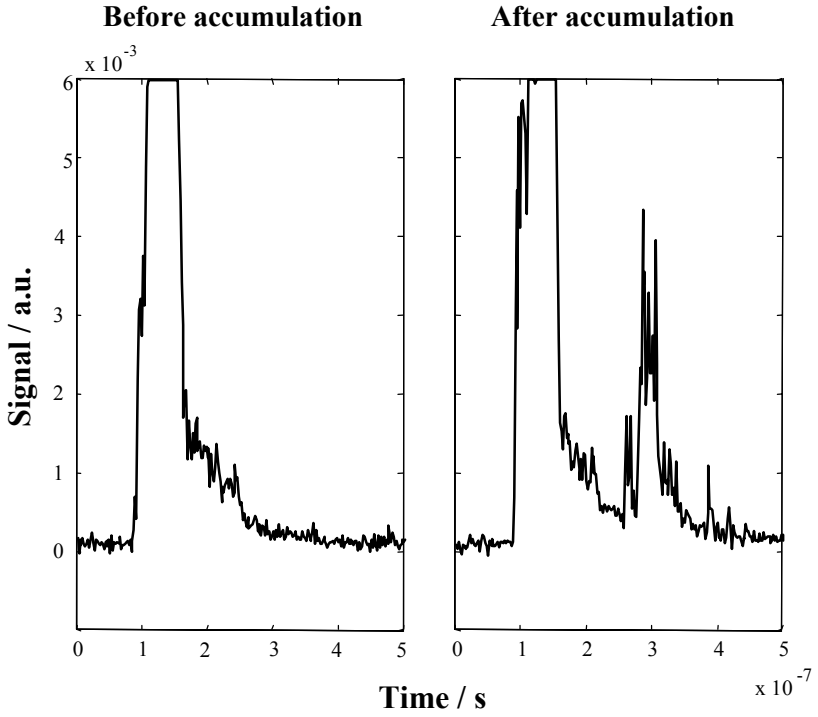

Figure 16. Signal obtained using excitation pulse pairs containing an average of 0.54 photons. The left part of the figure shows the result of a read-out before the accumulation sequence. The right part of the figure shows the signal obtained after the accumulation of $7{\cdot}10^9$ pulse pairs.

5.4. Comments on the experiment

The delayed single-photon self-interference experiment can be interpreted as a time domain analogue of the double slit experiment, but it can also be viewed as a pure photon echo experiment. Taking the latter view, it is interesting to note that the experiment indicates that it is possible to perform the three-pulse photon echo experiment with only a single photon (at a time) acting as two of the optical fields involved in the photon echo process. This is in contrast to some other non-linear optical processes, e.g. frequency doubling, where at least one photon per interaction is needed. This means that the arrows in the energy level diagrams often used to explain non-linear optical processes should not be interpreted as interactions with different photons.

The delayed single-photon self-interference experiment can also be viewed as a time domain version of Young's double slit experiment. In the double slit experiment, a transversal spatial modulation (the two slits) is transferred to an interference pattern when viewed in the Fourier plane of the slits (or in the optical far field). In the delayed single-photon self-interference experiment, a modulation in the time domain (the two pulses) is transferred to an interference pattern in the frequency domain, recorded by the ions in the crystal. One can argue that since the ions used as detectors in the experiment have a very narrow bandwidth, they will act as narrow-band filters and that this would mean that they will not have the temporal resolution to see the two excitation pulses. From this one might conclude that the two pulses actually do not exist, and that the ions in fact only experience one light pulse with a peculiar frequency content (corresponding to the Fourier transform of the two pulses). With this view, it is not so strange that the frequency content can be recorded by the ions in the crystal, since each ion only records the light at its specific absorption frequency. However, it is possible to transfer this view to the normal double slit experiment. In this case, the detector is placed in the Fourier plane of the two slits. If the detectors are small (spatially), they will only record a narrow band of spatial frequencies, and will therefore not be able to resolve the two slits. One would therefore have to conclude that the two slits do not exist and that the light hitting the detector merely has a somewhat peculiar modulation of its spatial frequencies. The magic in both of these experiments is revealed when a detector with a different bandwidth is used. If, in the double slit experiment, detectors that can resolve the two slits are used (this could be accomplished e.g. by moving the detectors closer to the slits), we see that the photon always travels through one of the slits and never through both of them simultaneously. If this is the case, the origin of the distribution of spatial frequencies recorded in the far field can not be explained easily. In the delayed single-photon self-interference experiment, one could use a detector with a large bandwidth (e.g. a fast photodiode), to conclude that a single photon will always be found in one of the two pulses, and never in both simultaneously. If this is really the case, the frequency pattern recorded by the ions in the photon echo material remains to be explained.

One way of circumventing the problems described above is to give up the notion of an objective reality and resort to a view where each experiment has to be analysed using the modes of the specific detector used in that experiment. This

means that we are only allowed to assign values to quantities that we can measure in a given experimental situation. Even if this view always seems to lead to the correct result regarding the outcome of experiments, many people (myself included) find it disturbing not to be able to tell what happens in each step of the experimental set-up without having to take the final method of detection into account.

Quantum mechanical interference experiments are often analysed in terms of "which-path" information. This means that if it is, even in principle, possible to extract information about which path the quantum object travelled to the detector, the interference pattern will be absent. It is therefore natural to analyse the delayed single-photon self-interference experiment in terms of which-path information. Naively, one would say that this experiment (especially in the way it was originally proposed with two spatially separated optical paths) indicates, in a rather direct way, that the photon actually travelled along both the possible paths, and that if it had taken only one of the paths, the signal would surely have disappeared. This is because the delay between the two paths is actually stored in the material, and this information can be extracted later as the arrival time of the echo signal. I, myself find it very difficult to explain how information about this delay can be transferred to the material if light did not propagate along both the possible paths to the material.

5.5. Related quantum optical experiments

In the experiment described in Paper III, a collinear geometry was used for the excitation pulses and the read-out pulse. This means that only the temporal part of the experiment originally suggested by Kessel and Moiseev was realised. However, it would still be interesting to do the original experiment with separate paths, since interference in both space and time would then be present in the same experiment. Also, if a very stable interferometer could be constructed, detecting the echo would probably be easier since the echo would be sent out in a direction different from that of the read-out pulse, which would make discrimination of the signal easier. This could make it possible to detect a signal at a lower excitation level, which would make it possible to attenuate the pulse pairs so as to contain a lower average photon number or to use shorter accumulation times before read-out.

In the original proposal for the delayed single-photon self-interference experiment, an experiment was also considered where interference could be observed without the accumulation of many pulse pairs. In this case, the read-out was proposed to take place after the interaction of a single photon with the photon echo material. The signal would then be built up by simply repeating the experiment several times and averaging the signal on the detection side. In this case, the signal (photon echo) has been predicted to have non-classical optical properties in that the expectation value of the intensity of the signal would be zero, whereas the electrical field would be non-zero.[64,71] Because of the non-linear

nature of the photon echo process, accumulation of several pulse pairs in the material before read-out is much more efficient in generating a signal than accumulating the signals from single pulse pairs, followed by read-out. For this reason, I believe that an experiment without accumulation would be very difficult to realise in practice. However, if no accumulation is to be performed, the optical properties of the photon echo material can be chosen more freely to render a higher efficiency for the photon echo process.

In other proposals, it has been suggested that the use of a three-level system, with the levels in a ladder configuration, would be advantageous for the experiment.[72] In this case, the pulse pairs would be resonant with the transition between the two lower lying levels, and the read-out pulse would be resonant with the transition between the two upper levels. In an experiment where only two levels are used, most of the atoms will be unaffected by the pulse pairs, and be left in their ground state. The strong read-out pulse will in this case excite these atoms, and the resulting fluorescence will constitute a background at the detector. However, in the three-level scheme, the read-out pulse will only interact with the atoms that were excited by the pulse pairs, which will reduce the background.

Using attenuated laser pulses, the quantum optical properties of the signal mentioned above will be washed out.[64] Ideally, single photon states should be used in the experiment, but due to the difficulties involved in generating single photon states experimentally, the use of squeezed states of light in the experiment is interesting since these states are easier to produce experimentally.[73]

The use of few-photon states in connection with photon echoes and rare-earth-ion-doped crystals has also been considered in the field of quantum state storage. In quantum information processing (see Chapter 6) it is often desirable to be able to store the quantum state of e.g. a photon in a medium and then to be able to recall a photon in the same state at a later time. Ultraslow and stopped light has been experimentally investigated in $Pr:Y_2SiO_5$ using electro-magnetically induced transparency (EIT).[74,75] Another proposal for quantum state storage is based on photon echoes in a three-level system of a Doppler-broadened optical transition in a gas.[76]

Another experiment that is related to the delayed single-photon self-interference experiment is one where microwave fields were used to produce a two-pulse spin echo from a single electron spin in a molecule.[77] In this experiment, a single molecule is exposed to microwaves representing first a $\pi/2$ pulse and then a π pulse for the electronic spin. The spin state of the molecule is then measured phase sensitively around the time when the spin echo is expected. The experiment is repeated a large number of times and the signal is taken as the sum of all the measurements. In this way, the normal ensemble of spins needed to produce the echo is replaced by a temporal average over all the measurements. Besides an average, inhomogeneous broadening is needed to produce an echo. For ensembles, this simply means that different members of the ensemble have different resonance frequencies. In the case of a single spin, the inhomogeneous broadening is created because, between measurements, the molecule undergoes a process which results in a random resonance frequency of the spin. This means that the spins in subsequent measurements will have

different resonance frequencies, and the inhomogeneous broadening is built up in the averaging of the different measurements.

6. Quantum information processing

The idea of using quantum mechanics in information processing was first put forward in 1980 by Benioff.[78] He showed that it was possible to build a classical Turing machine using quantum mechanics. This essentially means that using a quantum mechanical system, it is possible to solve all computational tasks that can be solved on a classical computer. The first person to indicate that the use of quantum mechanics could provide a computing device more powerful than classical physics could was R. Feynman.[79] He showed that a classical Turing machine could not efficiently simulate all quantum mechanical systems. He also indicated the possibility of a universal quantum simulator capable of simulating all other quantum mechanical systems efficiently. In 1985, D. Deutsch proposed the quantum Turing machine that could employ quantum parallelism to efficiently solve certain computational tasks.[80] The conjecture of Feynman in 1982 that quantum computers can efficiently simulate any (local) quantum system was finally proven in 1996.[81]

In this chapter, a brief introduction to quantum information processing will be give, followed by a short survey of a few of the many different physical systems that are being considered for the implementation of quantum information processing. The quantum computing scheme for rare-earth-ion-doped crystals presented in Paper IV and V is then described. The chapter ends with some reflections and considerations regarding the scheme.

6.1. Qubits and quantum gates

The basic building blocks in a classical computer are the bits and the gates. The quantum analogues are quantum bits (qubits) and quantum gates (for more elaborate descriptions of the ideas behind quantum computing see e.g. References 82-85). Qubits are made up of quantum mechanical two-level systems. As bits in a classical computer, qubits can take two values **0** and **1**, but as described in Chapter 2 of this thesis they can also form superpositions of the two states. It is in these superpositions that a large part of the power of quantum computers lies. This means that a quantum register with N quantum bits can be prepared in a state where all the numbers from $[0..2^N-1]$ are represented at the same time. This is in contrast to a register in a classical computer where only one

of these numbers can be represented at a time. The bits in a classical computer are manipulated using gates acting on the bits and, in an analogous way, quantum gates are used to manipulate the state of the qubits in a quantum computer. The gates can be divided into single-qubit gates, acting locally on a one qubit, and multiple-qubit gates which are used to perform conditional logic, i.e. when the state of one qubit should depend on the value of one or several other qubits. As for a classical computer, single-qubit-gates and gates involving two qubits are sufficient to perform any computation. To implement an arbitrary single qubit gate it must be possible to perform any rotation on the Bloch sphere representing the two qubit levels. As has been described in Chapter 2, this can be accomplished in optical systems by means of interactions with coherent light pulses, but many other means of manipulating qubits are also possible (see next section). Non-trivial two-qubit gates mean that the state of one of the qubits involved in the gate should be changed according to a rule which involves the state of the other qubit. The most commonly used example of a two-qubit gate is the Controlled-NOT (C-NOT) operation, which is the quantum analogue of the XOR gate in classical computers. To implement a C-NOT gate, the state of one of the qubits (the target qubit) should be swapped if and only if the state of the other qubit (the control qubit) is **1,** see Figure 17. It has been shown that the C-NOT gate is a universal gate for quantum computing, together with many other two-qubit gates.[86] This means that if the C-NOT gate can be implemented in combination with arbitrary single-qubit gates, all possible calculations can be described as combinations of these gates.

Input state		**Output state**	
Control	**Target**	**Control**	**Target**
|0>	|0>	|0>	|0>
|0>	|1>	|0>	|1>
|1>	|0>	|1>	|1>
|1>	|1>	|1>	|0>

Figure 17. Truth table for the Controlled-NOT gate where the state of the target bit is swapped if the control bit is in the |1> state.

Naively, it would seem that the use of superpositions and the entanglement created using quantum gates would make it possible to compute e.g. a function value for all possible input values simultaneously, which in a very easy way would constitute an exponential increase in speed compared with a classical computer. However, the situation is not quite that simple. When reading out the value of the qubits, quantum mechanics tells us that even though the qubits may contain information about a large number of computations that have been performed in parallel, at the time of the read-out the qubits will collapse into a single output value. To complicate things further, this value will be a random sample of all possible values, making the device non-deterministic. This means that it is in general not possible to simply use the algorithms that have been developed to work efficiently on classical computers on quantum computers.

Instead, special algorithms utilising the special features of quantum computers must be developed. So far, a rather limited number of quantum algorithms that can solve problems faster on a quantum computer than on a classical computer have been developed. I believe that one of the reasons for this is that to develop new efficient quantum algorithms, one must relinquish normal methods of solving problems. By this, I mean that the way in which we normally solve problems is based on actions that we could ourselves take in the physical world as we experience it, and that most phenomena we encounter in our everyday lives can be described by classical physics. However, some quantum algorithms that are more efficient (require fewer computational steps) than any corresponding classical algorithm have been developed. The one that has probably attracted most attention so far is Shor's algorithm for factoring.[2] This algorithm represents an exponential increase in speed compared with the best known classical algorithm. Another remarkable algorithm is Grover's search algorithm.[3] This algorithm deals with searching an unordered set, e.g. finding the name associated with a phone number by searching in the phone book. Using a classical algorithm, there is no better option than to start from the beginning of the phone book and check the phone numbers consecutively, which will mean that the number is found after checking, on the average, half of the numbers in the book. Grover's algorithm, on the other hand, uses quantum mechanical superpositions to perform the search, which means that only an average of the square root of the number of phone numbers must be checked before the correct phone number will be found. Apart from implementing quantum algorithms, a quantum computer could be used for efficiently simulating other quantum mechanical systems. Simulating quantum systems can not be done efficiently on classical computers, so quantum computers might be the only way for us to simulate complicated many-body quantum mechanical systems.

6.2. Physical systems

Quantum information processing has given rise to a new language when considering quantum mechanics. This enables people from different areas of physics to communicate using a common language. A large number of systems have been proposed as candidate systems for the experimental realisation of quantum gates. The systems and quantum computing schemes that I believe have the greatest similarities with the quantum-computing scheme in Paper IV will be briefly reviewed in this section.

6.2.1. Trapped ions

One of the first detailed schemes for the implementation of quantum computing was presented in 1995 by J. I. Cirac and P. Zoller.[87] In their scheme, a string of trapped cold ions constitutes the quantum computer. Two internal electronic states of the ions are used as the qubit states and each ion contains one qubit. Individual optical access to the ions is used for single qubit operations. Quantum gates involving any two ions in the string can be achieved using the collective motion of

the ions in the string. This collective motion can be excited using laser light if the laser is tuned off resonance with one of the ions by a frequency corresponding to a resonance frequency of the ion string. In this way, the motion can be excited provided that the ion at which the laser is directed is in a specific state. In this way, the state of any ion can be transferred to the state of the collective motion of the ions. In a similar way, the electronic state of another ion can be changed depending on the collective motion of all the ions. This mechanism enables coupling between qubits and makes conditional logic possible. A C-NOT gate, using the electronic state of one ion as one of the qubits and the motional state of the same ion as the other qubit, has been demonstrated in this system.[88] Scalability of the system is still an issue, but the demonstration of entanglement of four ions has shown that multi-ion gates might be possible.[89] This remarkable experiment was performed using a scheme where the cooling of the ions to their motional ground state is less critical than in the original scheme proposed by Cirac and Zoller.[90] Recently, a simple quantum algorithm (the Deutsch-Jozsa algorithm) has been implemented using the electronic and motional states of a single calcium ion.[91] Although scaling to many ions has proven to be non-trivial, grand plans exist for the construction of a large-scale ion-trap quantum computer.[92,93]

6.2.2. NMR

The quantum computing hardware in which the most complex qubit manipulations, in terms of the number of qubits and the number of gate operations, have been demonstrated so far, is liquid state NMR. The use of NMR for quantum computing was first proposed in 1997[94] and has since then made considerable experimental progress.[95] In this technique, the nuclear spins of spin-½ nuclei in molecules, in a static magnetic field are used as the qubits.[96] Single qubit operations are performed using RF pulses resonant with the precession frequency of the nucleus in the magnetic field. Different qubits can be addressed since they will have slightly different precession frequencies (chemical shifts) owing to their different positions in the molecule. Coupling between different qubits is possible since the precession frequency of one nucleus is sensitive to the spin of its neighbouring nuclei in the molecule. This means that if the state of one qubit is changed, the precession frequencies of the other qubits will change, which enables conditional logic to be performed between the qubits. Many of the proposed quantum algorithms have been tested using NMR, see e.g. References 97 and 98 and references therein. These tests have been performed on very simple input data, but have still provided very valuable demonstrations of both the algorithms and the experimental techniques. The most advanced demonstration so far is, in my opinion, the implementation of Shor's factoring algorithm using a molecule with seven qubits to factor the number 15, the simplest (non-trivial) instance of the problem.[99]

One problem that arises in NMR and many other systems is that the coupling between qubits can not be switched on and off. This means that qubits between which coupling exists, will be coupled to each other at all times. This causes problems when conditional logic is to be performed, since interaction is only desired between the qubits involved in the quantum gate. However, this can

be solved using refocusing pulses that remove the effect of unwanted qubits.[100] Another problem that arises in NMR is that when large molecules are used, not all qubits are positioned close enough to couple to each other. This makes it necessary to use a network of qubits, where interactions can be transferred between qubits. These and other issues make computations in NMR technically challenging, and pulse sequences consisting of hundreds of pulses are commonly used to implement the quantum algorithms. Another issue that been discussed in relation to NMR implementation of quantum information processing is the fact that the computations are not performed on single quantum systems as in e.g. ion traps, but an ensemble of a large number of molecules is used. Further, it is (so far) not possible to prepare the system in a pure state, with all quantum systems initially in the same state. Instead, the initial state is a thermal equilibrium state, which means that the lower energy state is only slightly more populated than the upper one. However, effective pure states can be extracted from thermal equilibrium states, and it is these states that constitute the qubits. The absence of pure initial states has made people question the "quantumness" of NMR implementation, leading to a, as yet, unresolved debate about what is really required from a physical system to gain the advantages of quantum computing over its classical counterpart, see e.g. References 101-103.

6.2.3. Solid state systems

Solid state realisation of quantum computers is generally thought to be easier to scale to large number of qubits than other systems. This is to a large extent due to the fact that these systems can often be manufactured using well-established techniques in lithography etc. However, because of the complexity of solid state devices and the non-negligible coupling between the qubits and the environment, it is often difficult to achieve long coherence times for the qubits in solid state materials.

A great deal of attention has recently been directed towards research on qubit realisation in superconducting circuits. Since this system is entirely man-made, using lithography, scaling to a large number of qubits is thought to be possible once the techniques for manipulating and coupling the qubits have been developed. If two small grains of superconducting material are coupled to each other with a Josephson tunnelling junction the (excess) charge of one of the grains can be used to form qubit states.[104] This means that the two qubit states are formed by the charge states corresponding to the existence or non-existence of one Cooper pair on the superconducting grain. Coherent oscillations have been observed between two different charge states on such a superconducting island.[105] Signs of entanglement between two qubits have also recently been reported.[106] One potential problem in using the charge as a qubit state is that since the qubit states are only separated by the charge corresponding to two electrons, the system is very sensitive to stray electric fields. These fields could originate from fluctuations in the applied voltages or fluctuations in the background charge distribution of the material surrounding the superconducting island. This makes it difficult, even at very low temperatures, to achieve long coherence times for the charge qubits.

Another quantum computing scheme for superconducting circuits is based on qubits consisting of persistent currents flowing in different directions in a superconducting circuit, so-called flux qubits.[107] Coherent superposition between the two states has been observed experimentally.[108,109] In these experiments, evidence of superposition of oppositely flowing currents of up to a few microamperes were observed. This superposition state differs from most other observed states, since it corresponds to the collective motion of millions of individual Cooper pairs, and makes this system interesting not only in the context of quantum information processing, but also in the exploration of the boundary between the microscopic and the macroscopic worlds. Flux qubits couple to the magnetic environment, but are insensitive to fluctuations in electric fields, which means that coherence times could potentially be longer than for charge qubits.

The best results so far in terms of coherence times for qubits in superconducting circuits have been obtained for circuits operating in a regime where the qubits are a combination of the two schemes described above.[110,111] In such systems, the superconducting circuits were operated in regimes where coupling to both the electric and the magnetic environments was minimised.

Another proposal that has attracted considerable attention is B. E. Cane's proposal of using the spins of phosphor atoms doped into pure silicon.[112] Single qubit gates are implemented using electrodes situated on top of each atom that can shift the resonance frequencies of the precessing spins. Interaction between qubits is due to exchange interactions between electrons. The strength of this interaction can be controlled by electrodes positioned between the atoms constituting the qubits. One attractive feature of this scheme is that the many methods developed in the semiconductor industry can be used in the realisation of the scheme. Another aspect is that efforts in this field will probably benefit the semiconductor industry, even if no quantum computer is ever built. A large consortium in Australia is currently exploring the possibility of realising this scheme, see e.g. Reference 113.

Schemes involving optical manipulation of solid state qubits include e.g. quantum dots.[114-116] In schemes using quantum dots as qubits, either spin states of the electrons or electron-hole pairs can be used as qubit states. These quantum states can then be manipulated using, for example, coherent light pulses, but other means of manipulation are also possible.

6.3. Rare-earth-ion-doped crystals for quantum information processing

In this section, some background information relevant to the quantum computing scheme presented in Paper IV will be given, together with some experimental data from initial experiments on the realisation of this scheme. In Paper IV, two different approaches were considered: one based on the use of a single ion for each qubit, and one where an ensemble of ions was used to form each qubit. In this section only the latter of the two approaches will be considered. This is due to the fact that the first approach requires the ability to detect single rare-earth ions.

Because of the low oscillator strengths of the rare-earth ions, this is a major experimental challenge, and has, to the best of the author's knowledge, not yet been accomplished. This type of single-molecule spectroscopy is also outside of the present expertise of our research group.

6.3.1. The qubits

In this scheme, it is proposed that the qubits be addressed in the frequency domain. This means that each qubit is defined by its absorption frequency on an inhomogeneously broadened optical transition. The qubit states are chosen so as to be two of the ground state hyperfine levels of the rare-earth ions. Single qubit gates can be achieved using resonant Raman pulses, meaning that the ions in the qubit are transferred between the qubit states via the optical transition.

The requirement on the ions in the scheme presented in Paper IV is that there exist three hyperfine levels in the ground state and one excited state. However, this is normally not the case for the rare-earth ions. At zero magnetic field, both praseodymium and europium have three non-degenerate hyperfine levels, both in the ground and excited states, which makes the quantum computing scheme more complicated. If the transition probabilities between the different hyperfine levels in the ground and excited states are not the same, different ions within the qubits will experience different pulse areas for the optical pulses involved in the Raman transitions. This is because within each frequency channel constituting a qubit, there will be ions for which that specific optical frequency corresponds to transitions to all different hyperfine levels in the excited state. This means that a single qubit gate will not place all ions within the qubit in the same qubit state, which would be detrimental for further computations. The transition probabilities between the hyperfine levels in the ground and excited states have been deduced from measurements on some materials.[117,118] These measurements indicate that the transitions can have quite different probabilities, at least for some combinations of dopant ions and host materials. However, the transition probabilities between the hyperfine levels in most combinations of dopants and host have yet to be measured. If materials in which the transition probabilities are different are to be used for the implementation of this scheme, this problem must be dealt with. This could possibly be done by further selection of the ions, so that only ions using the same excited state hyperfine levels in their transitions are used for the qubits. The other ions could be placed in the third hyperfine level of the ground state, called the auxiliary state. One way of achieving this would be by modifying the optical pumping scheme. Another way of selecting ions with a well-defined oscillator strength has been demonstrated experimentally using an ingenious scheme involving a sequence of pulses with pulse areas of 2π.[27] For ions with desired values of the oscillator strength, these pulses just rotate the state of the ions around one full circle on the Bloch sphere, but ions with other values of the oscillator strength will not end up in their ground state and will therefore eventually be transferred to another hyperfine state when the excited state decays.

A problem may arise if the transition from one of the qubit states to the upper state has a significantly different oscillator strength from that of the transition from this excited state down to the other qubit state. This would place

serious constraints on the laser source, since one of the optical fields involved in the Raman transition would have to be much more intense than the other, in order to compensate for the lower oscillator strength.

When implementing the single qubit gates, it is desirable that only the ions in the qubit are excited by the optical pulses, since spurious excitation of ions might lead to uncontrollable interactions between ions (see next section). This means that it is desirable to isolate the frequency channel used as the qubit from ions with absorption frequencies close to the qubit. This is described in Paper V, using optical pumping to create frequency intervals with (almost) no absorbing ions (called wells). The ions to be used as a qubit were then transferred back into the middle of the well, again using incoherent optical pumping. Another way of creating this type of structure is by means of coherent pulses.[27] By acting on the ions in the well with coherent optical pulses, it has been demonstrated that any superposition between the ground and optically excited states can be obtained and detected with high accuracy.[29]

In Figure 18 and Figure 19 two examples of qubit structures formed in rare-earth-ion-doped crystals can be seen. Figure 18 shows such a structure prepared using a ring dye laser in Eu:$YAlO_3$. Figure 19 shows the same type of structure for Tm:YAG placed in an external magnetic field. As reported in Paper II, Tm does not have any hyperfine splitting at zero magnetic field. When such a field is applied, the ground state is split into two hyperfine levels. Tm:YAG is not an obvious candidate for implementation of the quantum computing scheme since the scheme would have to be modified if only two hyperfine levels in the ground state can be used.

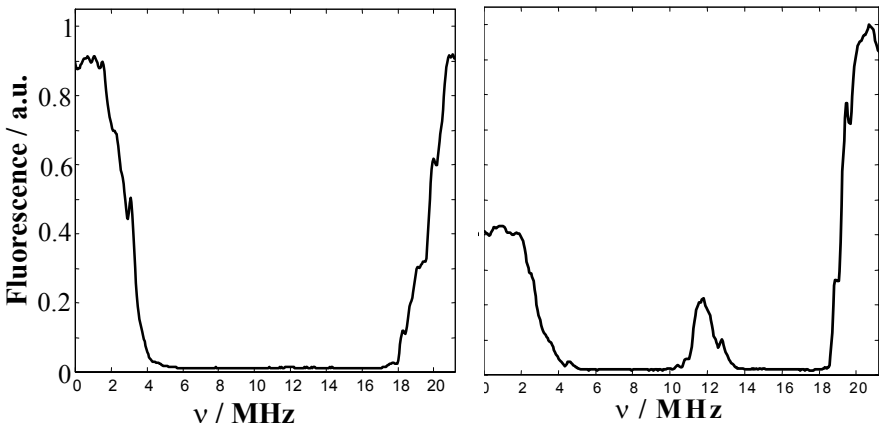

Figure 18. Qubit structure in Eu:$YAlO_3$ read out using fluorescence. The left curve shows a spectral well where all the ions have been removed by means of optical pumping and the right curve shows the qubit structure within the well.

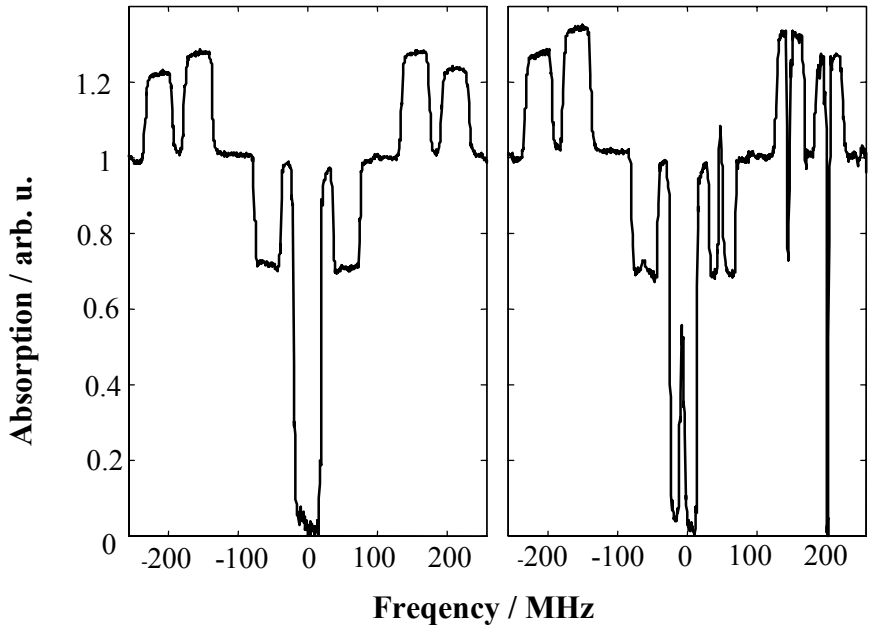

Figure 19. Qubit structure in Tm:YAG placed in an external magnetic field of 3 T. In the left part, a spectral well has been burnt in the absorption profile of the thulium ions (around zero MHz). The structure of holes and anti holes are due to the splitting of the ground and exited states in the magnetic field. In the right part of the figure, the laser has been tuned to around 200 MHz and a peak has been burnt back into the middle of the well. Please note that the data has been normalised and it is not certain that the absorption is zero in the middle of the well.

6.3.2. The interaction

For two-qubit quantum gates to be achieved, interaction between the qubits is necessary. In the rare-earth-ion-doped crystals, interaction between the ions can be accomplished using the difference in permanent electric dipole moment between the ground and excited states of the ions.[119,120] This means that the static electric field emanating from the ions will change when they are excited on the optical transition. This change in electric field will affect other ions that are situated close to the excited ion in the crystal, changing their absorption frequency, see Figure 20. The frequency change, $\Delta\nu$, for a neighbouring ion will be:

$$\Delta\nu = \frac{(\Delta\mu_1)(\Delta\mu_2)}{4\pi h\varepsilon\varepsilon_0 r^3}\left[(\hat{\mu}_1 \cdot \hat{\mu}_2) - 3(\hat{\mu}_1 \cdot \hat{r})(\hat{\mu}_2 \cdot \hat{r})\right] \qquad (6.1)$$

where $\Delta\mu$ is the difference in dipole moment between the ground and excited state (the indices 1 and 2 refer to the two ions involved in the process), h is Planck's

constant, ε_0 is the permittivity of vacuum, ε is the dielectric constant for the crystal and r is the distance between the two ions. $\hat{\mu}$ and $\hat{r}$ are unit vectors for the difference in dipole moments and the distance between the ions, respectively.

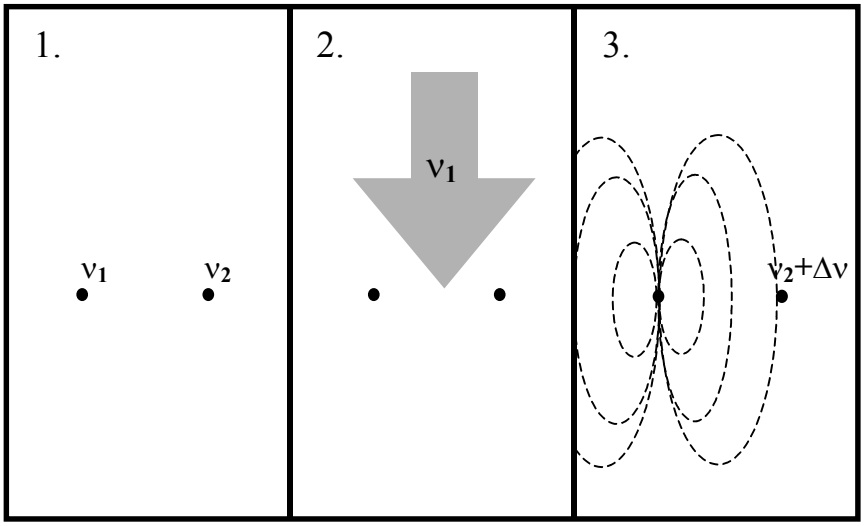

Figure 20. Schematic diagram showing the control mechanism between ions absorbing at different optical frequencies. 1. Two ions absorbing at different frequencies might be positioned close to each other in the crystal lattice. 2. By tuning the frequency of a laser to be in resonance with one of the ions, this ion can be transferred to its excited state. 3. When transferred to the excited state, the permanent dipole moment of the ion changes. This changes the electric field experienced by the other ion, causing a shift in the absorption frequency of this ion.

The dipole-dipole interaction described above can not immediately be used to construct quantum gates in rare-earth-ion-doped crystals. This is because the ions constituting each qubit are randomly positioned in the crystal, which means that the interaction between ions in different qubits will have different strengths owing to the different distances between the ions. However, if the frequency shifts imposed on the ions in one qubit upon the excitation of the ions in another qubit are greater than the width of the frequency wells in which the qubits are situated, quantum gates can readily be implemented for the two qubits (see Paper IV for more details). This means that if the ions within a qubit that are not shifted enough in frequency upon the excitation of another qubit can be removed, the remaining ions could be used in the implementation of a two-qubit gate. To accomplish this, an optical pumping scheme for the removal of the weakly interacting ions has been developed (see Paper IV). The crucial steps in this scheme are depicted in Figure 21, and result in two qubits containing only the ions between which the interaction is strong enough for quantum gates to be implemented.

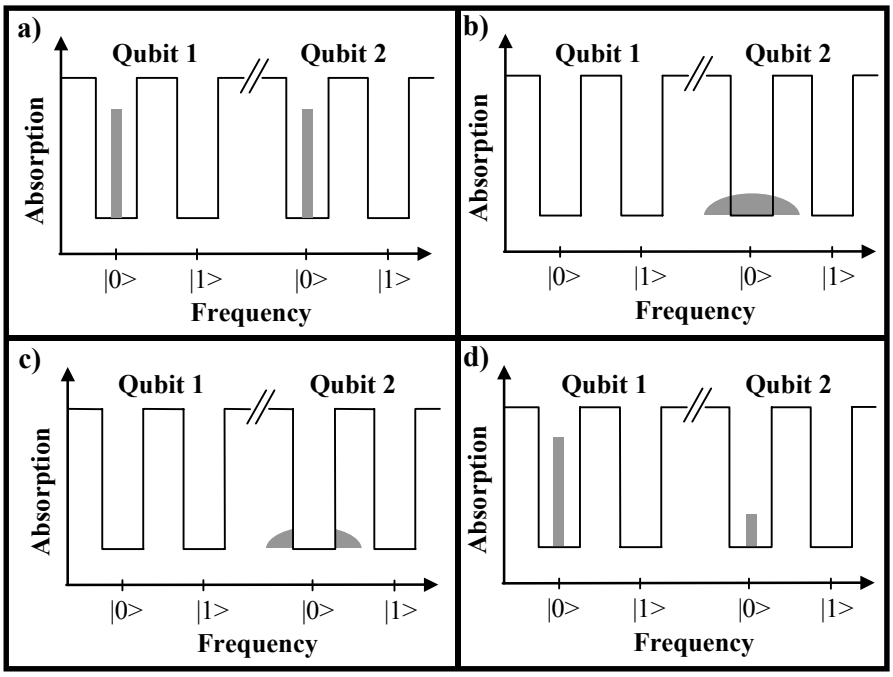

Figure 21. Schematic diagram of the procedure for selecting strongly interacting ions. a) Two qubit structures have been created and both qubits have been prepared in their |0> states. b) Qubit 1 is excited by an optical pulse. This shifts the absorption frequencies of the ions in qubit 2 and creates a distribution of frequencies for these ions. c) The ions belonging to qubit 2 which did not experience sufficient frequency shift upon the excitation of qubit 1 are moved to an auxiliary state using coherent optical pulses. d) The ions in qubit 1 are returned to their ground state and the remaining ions in qubit 2 thus return to their original frequencies. The result of the procedure is that quantum gates where qubit 1 is used to control the state of qubit 2 can be implemented.

An important aspect of this interaction mechanism is that it is only switched on when the ions are excited on the optical transition. This means that single-qubit gates can be implemented without taking into account the interaction between different qubits. It should be noted that apart from the electric dipole-dipole interaction described above, other static interaction mechanisms, such as that due to magnetic dipole moments, could also be used to implement the scheme. Excitation-induced interactions between rare-earth ions have been studied extensively in connection with photon echo experiments.[15] Interaction between ions has mainly been considered to be a problem, since it (seemingly) increases the homogeneous line width of the optical transition and thereby makes photon-echo-based data storage and processing more difficult to implement.

Numerical simulations have been performed to estimate the frequency shift imposed on the ions in one frequency channel upon the excitation of another frequency channel in a crystal where the ions are randomly positioned (see

Paper V). These simulations allow conclusions to be drawn about the number of ions that experience enough shift to be used in the implementation of a quantum gate. The numerical model that was used can be regarded as a Monte Carlo model, where the ions are placed at random positions in the crystal lattice, and the average field from all the ions is calculated. Several parameters, such as lattice constants, doping concentration, frequency channel width and difference in dipole moments of the ions can be varied to simulate different crystals and experimental conditions. The calculations are repeated for many probe ions in different positions in the lattice, resulting in a distribution of frequency shifts for the probe ions. This distribution mimics the different frequency shifts that are observed for ions in a real crystal.

A different way of using the dipole-dipole interaction mechanism from the one described above has been proposed.[29] In their study, the authors propose to use the photon echo process for selecting ions with appropriate interaction strengths. This method of selecting ions is claimed to result in larger number of ions that can be used when implementing the quantum gates.

6.4. Considerations relevant for a rare-earth-ion-based quantum computer

The coherence time for the hyperfine levels is an important parameter for the quantum computer scheme presented in Paper IV. For qubits not taking part in gate operations this time limits the time available for quantum computations. When the qubits are used in quantum gates, the phase memory for the optical transition is also important since the ions spend some of their time in the optically excited state. The coherence time for the hyperfine levels has been measured for $Pr:Y_2SiO_5$.[121,122] In another study, an external magnetic field was seen to increase the phase memory time for the hyperfine levels, and times as long as 82 ms have been reported.[123]

The rare-earth-ion-based quantum computing scheme is similar to NMR in that it does not provide access to individual quantum systems, but utilises ensembles for the computations. At the read-out stage, only the ensemble average of the qubit states can be read out. The information contained in the ensemble average can be quite different from that in the individual systems. However, the problem is not as severe as in NMR, since rare-earth ions can be prepared in the same initial state using e.g. optical pumping. This is, as yet, not possible in NMR, although some ingenious schemes have been developed to create larger differences between the qubit states before starting the computations.[124] It can be shown that in algorithms such as Shor's factoring algorithm, it is possible to extract the necessary information even if only an ensemble average is available.[85]

Ions with a distribution of different absorption frequencies are present within each frequency channel constituting a qubit, provided the frequency channels are broader in frequency than the homogeneous line width of the ions. This might be a problem when performing the gate operations as suggested in Paper IV, since the ions spend some of their time in the optically excited state.

Ions with different absorption frequencies will therefore acquire different phases, which will prevent further controlled interactions with the ions. A related problem will occur if the inhomogeneous broadening of the hyperfine levels is significant. In that case, this broadening must be taken into account for the individual qubits, but possibly also because the different qubits will acquire different phases when in superpositions between their qubit levels. Although the solution of these problems is not trivial, it seems reasonable to believe that the use of composite pulses, as in NMR, may be feasible.[125] Frequency selectivity and insensitivity to variations in the Rabi frequency (the transition probability between the hyper fine levels) can be accomplished using such composite pulses.[126]

The number of qubits that can be implemented with the scheme will be limited by the strength of the dipole-dipole interaction between the ions. This is because ions belonging to all the qubits must be situated close enough in the crystal in order for conditional logic between any pair of qubits to be possible. With the materials that have been considered in the present work, the number of qubits is likely to be limited to only a few. However, if a material doped with absorbers with a greater difference in dipole moment between their ground and excited states can be found, this number could be increased significantly.[127]

Many combinations of dopant ions and hosts can be considered for the implementation of quantum gates according to the scheme presented in Paper IV. It should be noted that most of the materials that have been investigated within this work have been developed to suit the requirements for use in data storage and processing applications. The requirements on materials intended for use in implementing quantum gates are quite different, and it might therefore be worthwhile to consider materials that have been rejected when considered for other applications. The quantum computing scheme might also be applied to crystals doped with transition elements or to NV centres in diamond.

Apart from the scheme presented in Paper IV, a few other schemes have been suggested for the realisation of quantum information processing in rare-earth-ion-doped crystals. In one of the schemes, use of the transition dipole moment is proposed for realising quantum gates between ions.[128] Further, the use of a magnetic field is proposed for shifting the frequency splitting of the ions to allow the gates to be implemented. In other schemes, it has been suggested that the coupling between ions, which is necessary for the implementation of quantum gates could be mediated by an optical cavity with a high Q value.[129,130]

Acknowledgements

First of all, I would like to thank my main supervisor Stefan Kröll for guiding me through this project and for always taking time to help me with the problems I have encountered. I am especially grateful to him for giving me the opportunity to meet and work with scientists from all over the world, and for always encouraging me to broaden my knowledge in physics. I am also grateful to my other supervisor, Sune Svanberg, for his never-ending enthusiasm and help.

Furthermore, I would like to thank all the people who have worked in the photon echo group at the Division of Atomic Physics for creating a helpful and open atmosphere. I would especially like to thank Krishna Mohan for interesting discussions about physics as well as life, philosophy, Indian culture and cricket. My roommate, Lars Rippe, has been a good friend and colleague, always ready to tackle any problem over a cup of coffee. I am also grateful to Mattias Nilsson for his friendship and support. His company made the long nights spent in the lab much more fun.

I have enjoyed working in the friendly environment at the Division of Atomic Physics. Magnus, Petter, Johan, Anders, Ola, Allan and others have all helped in creating a pleasant atmosphere. I would also like to thank Åke Bergquist and Bertil Hermansson for always being patient and answering my ignorant questions regarding electronics and computers. The help of Laila Lewin, Marie Holmdahl-Svensson and Britt-Marie Hansson is also much appreciated. I would also like to express special thanks to Leif Magnusson for his generous help with the cryogenics.

I would like to thank everyone at the teaching department for giving me the opportunity to improve as a teacher. I would especially like to thank Nina Reistad, Lars Engström and Lennart Nilsson for their friendly collaboration.

I have had the privilege of working with Serguei Moiseev during his visits to Sweden. Our bowling and chess games are experiences that will definitely be remembered.

I would like to thank my family and friends for the support and encouragement they have given me. My parents have always urged me to make my own decisions, and have stood behind me as I have done so. Johan, my brother, has helped me to put things into perspective when necessary.

Finally, I would like to thank my girlfriend Cecilia. Du är bäst!

Summary of the papers

Paper I describes an experiment where frequency-chirped laser pulses from an external cavity diode laser were temporally compressed in a photon echo process. Compression by a factor of 450 was achieved for single pulses. Multi-pulse compression was investigated, and theoretical expressions for the pulse shapes of the compressed pulses were obtained and compared with the experimental data.

I took part in some of the experimental and theoretical work that led to the paper.

Paper II reports on a long-time storage mechanism for thulium ions doped into YAG when an external magnetic field is applied. Storage times of spectral features in the material of several tens of seconds were obtained, which is several orders of magnitude longer than that achieved without an external magnetic field. The mechanism enabling the long storage time is the magnetic-field-induced splitting of the ground state into two hyperfine levels. The splitting of the levels in the ground and excited states was investigated as a function of the applied magnetic field for field strengths up to 5 T.

I participated in all the experiments and data evaluation. I also wrote the manuscript.

Paper III presents an accumulated photon echo experiment in which the excitation pulses were attenuated so as to contain less than one photon on average. At such low light levels, effects due to the quantisation of the electromagnetic field have to be taken into account. The signal strengths obtained are compared with theoretical predictions both for the case when at least one photon is required in each of the excitation pulses and for the case when one photon can be shared between the two pulses. The experimental data seem to support the suggestion that a single photon can act as two of the optical fields involved in the photon echo process.

I designed the experiment for demonstrating the proposed idea and was the main responsible for the experimental work and the data analysis. I also wrote the manuscript.

Paper IV describes a scheme for the implementation of quantum gates in rare-earth-ion-doped crystals. It is proposed that the individual qubits are formed using two of the hyperfine levels of the ions. Different ions can be addressed using their different absorption frequencies on an inhomogeneously broadened optical transition. Coupling between different qubits, enabling the implementation of quantum gates, is achieved using the dipole-dipole interaction between ions in the crystal. Further, a method for selecting groups of ions where this interaction has sufficient strength is presented. This enables working quantum computers to be extracted from the randomly positioned ions in the crystal.

I contributed to the development of the scheme presented in the paper. In particular, I developed the method of selecting strongly interacting ions. I also wrote the manuscript.

Paper V describes the first steps in assessing the viability of the scheme presented in Paper IV. Ions absorbing within a narrow frequency channel were prepared in one of the qubit states. Interaction between different frequency channels was observed and compared with predictions from numerical simulations.

I was responsible for the numerical simulations of interaction between ions. I participated in the planning of the experiments and wrote part of the manuscript.

References

1. T. H. Maiman, "Stimulated optical radiation in ruby.," Nature **187,** 493 (1960).

2. P. W. Shor, "Polynomial-time algorithms for prime factorization and discrete logarithms on a quantum computer," Siam J. Comput **26,** 1484-1509 (1997).

3. L. K. Grover, "Quantum mechanics helps in searching for a needle in a haystack," Phys. Rev. Lett. **79,** 325-328 (1997).

4. M. O. Scully and M. S. Zubairy, *Quantum Optics*, (Cambridge University Press, 1997).

5. R. W. Boyd, *Nonlinear Optics*, (Academic press limited, London, England, 1992).

6. R. L. Shoemaker, "Coherent Transient Infrared Spectroscopy," in *Laser and Coherence Spectroscopy,* J. I. Steinfeld (ed.), (Plenum Press, New York, 1978), pp. 197-371 .

7. S. L. McCall and E. L. Hahn, "Self-Induced Transparency by Pulsed Coherent Light," Phys. Rev. Lett. **18,** 908-912 (1967).

8. R. M. Macfarlane and R. M. Shelby, "Coherent transient and holeburning spectroscopy of rare earth ions in solids," in *Spectroscopy of Solids Containing Rare Earth Ions,* Kaplyanskii A.A. and R. M. Macfarlane (eds.), (North-Holland, Amsterdam, 1987).

9. W. E. Moerner, K. K. Rebane, L. A. Rebane, D. Haarer, R. M. Macfarlane, R. M. Shelby, J. M. Hayes, R. Jankowiak, G. J. Small, A. J. Sievers, W. Lenth, and G. C. Bjorklund, *Persistent Spectral Hole-Burning: Science and Applications*, (Springer-Verlag, Berlin, 1988).

10. B. Henderson and G. F. Imbush, *Optical Spectroscopy of Inorganic Solids*, (Clarendon Press, Oxford, 1989).

11. R. M. Macfarlane, "High-resolution laser spectroscopy of rare-earth doped insulators: a personal perspective," J. Lumin. **100,** 1-20 (2002).

12. R. W. Equall, Y. Sun, R. L. Cone, and R. M. Macfarlane, "Ultraslow optical dephasing in Eu^{3+}:Y_2SiO_5," Phys. Rev. Lett. **72,** 2179-2181 (1994).

13. Y. Sun, C. W. Thiel, R. L. Cone, R. W. Equall, and R. L. Hutcheson, "Recent progress in developing new rare earth materials for hole burning and coherent transient applications," J. Lumin. **98,** 281-287 (2002).

14. A. Caprez, P. Meyer, P. Mikhail, and J. Hulliger, "New host-lattices for hyperfine optical hole burning: Materials of low nuclear spin moment," Mater. Res. Bull. **32,** 1045-1054 (1997).

15. S. Kröll, E. Y. Xu, and R. Kachru, "Influence of Excited-State Pr3+ On the Relaxation of the Pr^{3+}:$YAlO_3$ $^3H_4$-$^1D_2$ Transition," Phys. Rev. B **44,** 30-34 (1991).

16. S. B. Altner, G. Zumofen, U. P. Wild, and M. Mitsunaga, "Photon-echo attenuation in rare-earth-ion-doped crystals," Phys. Rev. B **54,** 17493-17507 (1996).

17. M. Mitsunaga, T. Takagahara, R. Yano, and N. Uesugi, "Excitation-induced frequency shift probed by stimulated photon echoes," Phys. Rev. Lett. **68,** 3216-3219 (1992).

18. F. R. Graf, A. Renn, G. Zumofen, and U. P. Wild, "Photon-echo attenuation by dynamical processes in rare-earth- ion-doped crystals," Phys. Rev. B **58,** 5462-5478 (1998).

19. G. J. Pryde, T. Bottger, R. L. Cone, and R. C. C. Ward, "Semiconductor lasers stabilized to spectral holes in rare earth crystals to a part in 10(13) and their application to devices and spectroscopy," J. Lumin. **98,** 309-315 (2002).

20. P. B. Sellin, N. M. Strickland, T. Bottger, J. L. Carlsten, and R. L. Cone, "Laser stabilization at 1536 nm using regenerative spectral hole burning," Phys. Rev. B **6315,** art-155111 (2001).

21. A. M. Stoneham, "Shapes of Inhomogeneously Broadened Resonance Lines in Solids," Reviews Of Modern Physics **41,** 82-108 (1969).

22. M. Yamaguchi, K. Koyama, T. Suemoto, and M. Mitsunaga, "Perturbed ion sites in Eu^{3+}:$YAlO_3$ studied by optical-rf double-resonance spectroscopy," Phys. Rev. B **59,** 9126-9131 (1999).

23. L. Levin, "Mode-hop-free electro-optically tuned diode laser," Opt. Lett. **27,** 237-239 (2002).

24. E. L. Hahn, "Spin Echoes," Phys. Rev. **80,** 580-594 (1950).

25. N. A. Kurnit, S. R. Hartmann, and I. D. Abella, "Observation of Photon Echo," Phys. Rev. Lett. **13,** 567-568 (1964).

26. I. D. Abella, N. A. Kurnit, and S. R. Hartmann, "Photon echoes," Phys. Rev. **141,** 391-406 (1966).

27. G. J. Pryde, M. J. Sellars, and N. B. Manson, "Solid state coherent transient measurements using hard optical pulses," Phys. Rev. Lett. **84,** 1152-1155 (2000).

28. G. J. Pryde, M. J. Sellars, and N. B. Manson, "Optical non-Bloch behaviour observed using an optical Carr-Purcell-Meiboom-Gill pulse sequence," J. Lumin. **86,** 279-283 (2000).

29. J. J. Longdell and M. J. Sellars, "Experimental demonstration of quantum state tomography applied to dopant ions in a solid," quant-ph/ 0208182 (2002).

30. A. V. Durrant, J. Manners, and P. M. Clark, "Understanding optical echoes using Schrödinger's equation: I. Echoes excited by two optical pulses," Eur. J. Phys. **10,** 291-297 (1989).

31. R. Beach, S. R. Hartmann, and R. Friedberg, "Billiard-ball echo model," Phys. Rev. A **25,** 2658-2666 (1982).

32. M. Mitsunaga, "Time-Domain Optical-Data Storage By Photon-Echo," Opt. Quant. Electron. **24,** 1137-1150 (1992).

33. A. V. Durrant, J. Manners, and P. M. Clark, "Understanding optical echoes using Schrödinger's equation: II. Three pulse echoes and collision effects," Eur. J. Phys. **12,** 234-239 (1991).

34. S. Kröll and P. Tidlund, "Recording density limit of photon-echo optical storage with high-speed writing and reading," Appl. Opt. **32,** 7233-7242 (1993).

35. T. W. Mossberg, R. Kachru, and S. R. Hartmann, "Echoes in gaseous media - generalized theory of rephasing phenomena," Phys. Rev. A **20,** 1976-1996 (1979).

36. J. B. W. Morsink, W. H. Hesselink, and D. A. Wiersma, "Photon-echo stimulated from optically induced nuclear-spin polarization," Chem. Phys. Lett. **64,** 1-4 (1979).

37. M. K. Kim and R. Kachru, "Multiple-bit long-term data-storage by backward-stimulated echo in Eu^{3+}:$YAlO_3$," Opt. Lett. **14,** 423-425 (1989).

38. M. Mitsunaga, R. Yano, and N. Uesugi, "Spectrally programmed stimulated photon echo," Opt. Lett. **16,** 264-266 (1991).

39. V. A. Zuikov, V. V. Samartsev, and R. G. Usmanov, "Correlation of the shape of light-echo signals with the shape of the excitation pulses," JETP Letters **32,** 270-274 (1980).

40. T. W. Mossberg, "Time-domain frequency-selective optical-data storage," Opt. Lett. **7,** 77-79 (1982).

41. A. G. Anderson, R. L. Garwin, E. L. Hahn, J. W. Horton, G. L. Tucker, and R. M. Walker, "Spin echo serial storage memory," J. Appl. Phys. **26,** 1324-1338 (1955).

42. W. R. Babbitt and T. W. Mossberg, "Quasi-2-dimensional time-domain color memories - process limitations and potentials," J. Opt. Soc. Am. B **11,** 1948-1953 (1994).

43. T. W. Mossberg, "Swept-carrier time-domain optical memory," Opt. Lett. **17,** 535-537 (1992).

44. H. Lin, T. Wang, and T. W. Mossberg, "Demonstration of 8 Gbit/in.^{2} areal storage density based on swept-carrier frequency-selective optical memory," Opt. Lett. **20,** 1658-1660 (1995).

45. L. Menager, J. L. Le Gouet, and I. Lorgere, "Time-to-frequency Fourier transformation with photon echoes," Opt. Lett. **26,** 1397-1399 (2001).

46. K. D. Merkel and W. R. Babbitt, "Optical coherent-transient true-time-delay regenerator," Opt. Lett. **21,** 1102-1104 (1996).

47. M. Z. Tian, R. Reibel, and W. R. Babbitt, "Demonstration of optical coherent transient true-time delay at 4 Gbits/s," Opt. Lett. **26,** 1143-1145 (2001).

48. K. D. Merkel, R. D. Peters, P. B. Sellin, K. S. Repasky, and W. R. Babbitt, "Accumulated programming of a complex spectral grating," Opt. Lett. **25,** 1627-1629 (2000).

49. K. D. Merkel and W. R. Babbitt, "Chirped-pulse programming of optical coherent transient true-time delays," Opt. Lett. **23,** 528-530 (1998).

50. W. R. Babbitt and T. W. Mossberg, "Spatial routing of optical beams through time-domain spatial-spectral filtering," Opt. Lett. **20,** 910-912 (1995).

51. H. Lin, T. Wang, G. A. Wilson, and T. W. Mossberg, "Experimental demonstration of swept-carrier time-domain optical memory," Opt. Lett. **20,** 91-93 (1995).

52. X. A. Shen and R. Kachru, "Optical header recognition by spectroholographic filtering," Opt. Lett. **20,** 2508-2510 (1995).

53. T. L. Harris, Y. Sun, R. L. Cone, R. M. Macfarlane, and R. W. Equall, "Demonstration of real-time address header decoding for optical data routing at 1536 nm," Opt. Lett. **23,** 636-638 (1998).

54. Y. S. Bai and T. W. Mossberg, "Photon-echo optical pulse-compression," Appl. Phys. Lett. **45,** 1269-1271 (1984).

55. Y. S. Bai and T. W. Mossberg, "Experimental studies of photon-echo pulse-compression," Opt. Lett. **11,** 30-32 (1986).

56. F. R. Graf, B. H. Plagemann, E. S. Maniloff, S. B. Altner, A. Renn, and U. P. Wild, "Data compression in frequency-selective materials using frequency-swept excitation pulses," Opt. Lett. **21,** 284-286 (1996).

57. T. Wang, H. Lin, and T. W. Mossberg, "Optical bit-rate conversion and bit-stream time-reversal by the use of swept-carrier frequency-selective optical-data storage techniques," Opt. Lett. **20,** 2033-2035 (1995).

58. B. Luo, U. Elman, S. Kröll, R. Paschotta, and A. Tropper, "Amplification of photon echo signals by use of a fiber amplifier," Opt. Lett. **23,** 442-444 (1998).

59. R. K. Mohan, U. Elman, M. Z. Tian, and S. Kröll, "Regeneration of photon echoes with amplified photon echoes," Opt. Lett. **24,** 37-39 (1999).

60. Z. W. Barber, M. X. Tian, R. R. Reibel, and W. R. Babbitt, "Optical pulse shaping using optical coherent transients," Opt. Express **10,** 1145-1150 (2002).

61. R. P. Feynman, R. B. Leighton, and M. Sands, *The Feynman Lectures on Physics, Volume III*, (Addison-Wesley Publishing Company, 1965).

62. P. A. M. Dirac, "The Quantum Theory of the Emission and Absorption of Radiation," Proceedings Of The Royal Society Of London Series A-Mathematical And Physical Sciences **114,** 243-265 (1927).

63. A. R. Kessel and S. A. Moiseev, "Delayed Self-Interference of a Photon," JETP Letters **58,** 80-84 (1993).

64. R. Friedberg and S. R. Hartmann, "Photon/Zen echoes," Laser Phys. **9,** 1083-1101 (1999).

65. R. K. Mohan, B. Luo, S. Kröll, and A. Mair, "Delayed single-photon self-interference," Phys. Rev. A **58,** 4348-4358 (1998).

66. T. Reinot, W. H. Kim, J. M. Hayes, and G. J. Small, "New standard for high-temperature persistent-hole-burning molecular materials: Aluminum phthalocyanine tetrasulphonate in buffered hyperquenched glassy films of water," J. Opt. Soc. Am. B **14,** 602-608 (1997).

67. M. J. Sellars, Private communications (2000).

68. K. Holliday, M. Croci, E. Vauthey, and U. P. Wild, "Spectral hole-burning and holography in an $Y_2SiO_5:Pr^{3+}$ crystal," Phys. Rev. B **47,** 14741-14752 (1993).

69. R. Saers, *Stabilising a Ring Dye Laser to Iodine Transitions*, (Lund Reports on Atomic Physics, LRAP-282, Diploma paper, Lund, Sweden, 2002).

70. Y. C. Chen, K. Chiang, and S. R. Hartmann, "Spectroscopic and relaxation character of the $^3P_0$-$^3H_4$ transition in $LaF_3:Pr^{3+}$ measured by photon echoes," Phys. Rev. B **21,** 40-47 (1980).

71. S. A. Moiseev, "Time-Delayed Interference of a Photon and the One-Photon Echo in media with Phase Memory," Optics and Spectroscopy **83,** 280-294 (1997).

72. S. A. Moiseev, "Time-delayed quantum interference and single-photon echo in coherent three-level systems," Quantum Electronics **31,** 557-563 (2001).

73. S. A. Moiseev, "Effects of wave function reduction in a one-photon echo," Optics and Spectroscopy **84,** 717-723 (1998).

74. B. S. Ham, P. R. Hemmer, and M. S. Shahriar, "Efficient electromagnetically induced transparency in a rare- earth doped crystal," Opt. Commun. **144,** 227-230 (1997).

75. A. V. Turukhin, V. S. Sudarshanam, M. S. Shahriar, J. A. Musser, B. S. Ham, and P. R. Hemmer, "Observation of ultraslow and stored light pulses in a solid," Phys. Rev. Lett. **88,** art-023602 (2002).

76. S. A. Moiseev and S. Kröll, "Complete reconstruction of the quantum state of a single-photon wave packet absorbed by a Doppler-broadened transition," Phys. Rev. Lett. **87,** art-173601 (2001).

77. J. Wrachtrup, C. von Borczyskowski, J. Bernard, R. Brown, and M. Orrit, "Hahn echo experiments on a single triplet electron spin," Chem. Phys. Lett. **245,** 262-267 (1995).

78. P. Benioff, "The Computer as a Physical System - A Microscopic Quantum-Mechanical Hamiltonian Model of Computers as Represented by Turing-Machines," Journal of Statistical Physics **22,** 563-591 (1980).

79. R. P. Feynman, "Simulating Physics with Computers," International Journal of Theoretical Physics **21,** 467-488 (1982).

80. D. Deutch, "Quantum-Theory, The Church-Turing Principle and the Universal Quantum Computer," Proceedings Of The Royal Society of London Series A- Mathematical Physical And Engineering Sciences **400,** 97-117 (1985).

81. S. Lloyd, "Universal quantum simulators," Science **273,** 1073-1078 (1996).

82. A. Steane, "Quantum computing," Rep. Prog. Phys. **61,** 117-173 (1998).

83. C. H. Bennett and P. W. Shor, "Quantum information theory," IEEE Transactions On Information Theory **44,** 2724-2742 (1998).

84. C. P. Williams and S. H. Clearwater, *Explorations in Quantum Computing*, (Springer-Verlag New York, 1998).

85. M. A. Nielsen and I. L. Chuang, *Quantum Computation and Quantum Information*, (Cambridge University Press, 2000).

86. A. Barenco, C. H. Bennett, R. Cleve, D. P. DiVincenzo, N. Margolus, P. Shor, T. Sleator, J. A. Smolin, and H. Weinfurter, "Elementary gates for quantum computation," Phys. Rev. A **52,** 3457-3467 (1995).

87. J. I. Cirac and P. Zoller, "Quantum Computations with Cold Trapped Ions," Phys. Rev. Lett. **74,** 4091-4094 (1995).

88. C. Monroe, D. M. Meekhof, B. E. King, W. M. Itano, and D. J. Wineland, "Demonstration of a Fundamental Quantum Logic Gate," Phys. Rev. Lett. **75,** 4714-4717 (1995).

89. C. A. Sackett, D. Kielpinski, B. E. King, C. Langer, V. Meyer, C. J. Myatt, M. Rowe, Q. A. Turchette, W. M. Itano, D. J. Wineland, and I. C. Monroe, "Experimental entanglement of four particles," Nature **404,** 256-259 (2000).

90. K. Molmer and A. Sorensen, "Multiparticle entanglement of hot trapped ions," Phys. Rev. Lett. **82,** 1835-1838 (1999).

91. S. Gulde, M. Riebe, G. P. T. Lancaster, C. Becher, J. Eschner, H. Häffner, F. Schmidt-Kaler, I. L. Chuang, and R. Blatt, "Implementation of the Deutsch-Jozsa algorithm on an ion-trap quantum computer," Nature **421,** 48-50 (2003).

92. D. Kielpinski, C. Monroe, and D. J. Wineland, "Architecture for a large-scale ion-trap quantum computer," Nature **417,** 709-711 (2002).

93. A. Sorensen and K. Molmer, "Quantum computation with ions in thermal motion," Phys. Rev. Lett. **82,** 1971-1974 (1999).

94. D. G. Cory, A. F. Fahmy, and T. F. Havel, "Ensemble quantum computing by NMR spectroscopy," Proceedings of The National Academy of Sciences of The United States of America **94,** 1634-1639 (1997).

95. N. A. Gershenfeld and I. L. Chuang, "Bulk spin-resonance quantum computation," Science **275,** 350-356 (1997).

96. M. Steffen, L. M. K. Vandersypen, and I. L. Chuang, "Toward quantum computation: A five-qubit quantum processor," IEEE Micro **21,** 24-34 (2001).

97. C. H. Bennett and D. P. DiVincenzo, "Quantum information and computation," Nature **404,** 247-255 (2000).

98. J. A. Jones, "NMR quantum computation," Progress In Nuclear Magnetic Resonance Spectroscopy **38,** 325-360 (2001).

99. L. M. K. Vandersypen, M. Steffen, G. Breyta, C. S. Yannoni, M. H. Sherwood, and I. L. Chuang, "Experimental realization of Shor's quantum factoring algorithm using nuclear magnetic resonance," Nature **414,** 883-887 (2001).

100. D. W. Leung, I. L. Chuang, F. Yamaguchi, and Y. Yamamoto, "Efficient implementation of coupled logic gates for quantum computation," Phys. Rev. A **6104,** art-042310 (2000).

101. R. Laflamme, D. Cory, C. Negrevergne, and L. Viola, "NMR quantum information processing and entanglement," Quantum Information & Computation **2,** 166-176 (2002).

102. S. L. Braunstein, C. M. Caves, R. Jozsa, N. Linden, S. Popescu, and R. Schack, "Separability of very noisy mixed states and implications for NMR Quantum computing," Phys. Rev. Lett. **83,** 1054-1057 (1999).

103. A. Ekert and R. Jozsa, "Quantum algorithms: entanglement-enhanced information processing," Philosophical Transactions of The Royal Society of London Series A-Mathematical Physical and Engineering Sciences **356,** 1769-1781 (1998).

104. A. Shnirman, G. Schon, and Z. Hermon, "Quantum manipulations of small Josephson junctions," Phys. Rev. Lett. **79,** 2371-2374 (1997).

105. Y. Nakamura, Y. A. Pashkin, and J. S. Tsai, "Coherent control of macroscopic quantum states in a single-Cooper-pair box," Nature **398,** 786-788 (1999).

106. Y. A. Pashkin, T. Yamamoto, O. Astafiev, Y. Nakamura, D. V. Averin, and J. S. Tsai, "Quantum oscillations in two coupled charge qubits," Nature **421,** 823-826 (2003).

107. J. E. Mooij, T. P. Orlando, L. Levitov, L. Tian, C. H. van der Wal, and S. Lloyd, "Josephson persistent-current qubit," Science **285,** 1036-1039 (1999).

108. C. H. van der Wal, A. C. J. ter Haar, F. K. Wilhelm, R. N. Schouten, C. J. P. M. Harmans, T. P. Orlando, S. Lloyd, and J. E. Mooij, "Quantum superposition of macroscopic persistent-current states," Science **290,** 773-777 (2000).

109. J. R. Friedman, V. Patel, W. Chen, S. K. Tolpygo, and J. E. Lukens, "Quantum superposition of distinct macroscopic states," Nature **406,** 43-46 (2000).

110. D. Vion, A. Aassime, A. Cottet, P. Joyez, H. Pothier, C. Urbina, D. Esteve, and M. H. Devoret, "Manipulating the quantum state of an electrical circuit," Science **296,** 886-889 (2002).

111. Y. Yu, S. Y. Han, X. Chu, S. I. Chu, and Z. Wang, "Coherent temporal oscillations of macroscopic quantum states in a Josephson junction," Science **296,** 889-892 (2002).

112. B. E. Kane, "A silicon-based nuclear spin quantum computer," Nature **393,** 133-137 (1998).

113. J. L. O'Brien, S. R. Schofield, M. Y. Simmons, R. G. Clark, A. S. Dzurak, N. J. Curson, B. E. Kane, N. S. McAlpine, M. E. Hawley, and G. W. Brown, "Towards the fabrication of phosphorus qubits for a silicon quantum computer," Phys. Rev. B **6416,** art-161401 (2001).

114. G. D. Sanders, K. W. Kim, and W. C. Holton, "Optically driven quantum-dot quantum computer," Phys. Rev. A **60,** 4146-4149 (1999).

115. A. Imamoglu, D. D. Awschalom, G. Burkard, D. P. DiVincenzo, D. Loss, M. Sherwin, and A. Small, "Quantum information processing using quantum dot spins and cavity QED," Phys. Rev. Lett. **83,** 4204-4207 (1999).

116. G. D. Sanders, K. W. Kim, and W. C. Holton, "Scalable solid-state quantum computer based on quantum dot pillar structures," Phys. Rev. B **61,** 7526-7535 (2000).

117. J. J. Longdell, M. J. Sellars, and N. B. Manson, "Hyperfine interaction in ground and excited states of praseodymium-doped yttrium orthosilicate," Phys. Rev. B **66,** art-035101 (2002).

118. T. Blasberg and D. Suter, "Determination of oscillator strengths in Pr^{3+}:$YAlO_3$ by Raman heterodyne and hole burning spectroscopy," J. Lumin. **65,** 199-209 (1995).

119. A. J. Meixner, C. M. Jefferson, and R. M. Macfarlane, "Measurement of the Stark effect with subhomogeneous linewidth resolution in Eu^{3+}:$YAlO_3$ with the use of photon-echo modulation," Phys. Rev. B **46,** 5912-5916 (1992).

120. F. R. Graf, "Investigation of spectral dynamics in rare earth ion doped crystals using high resolution laser techniques," (1998). PhD Thesis, ETH Zürich.

121. B. S. Ham, M. S. Shahriar, M. K. Kim, and P. R. Hemmer, "Spin coherence excitation and rephasing with optically shelved atoms," Phys. Rev. B **58,** R11825-R11828 (1998).

122. F. Vestin, *Spin Coherence Excitation in* $Pr^{3+}:Y_2SiO_5$, (Lund Reports on Atomic Physics, LRAP-297, Diploma paper, Lund, Sweden, 2003).

123. A. Alexander, *Investigation of Qubit Isolation in a Rare-Earth Quantum Computer*, (Honour Thesis, Department of Physics, The Australian National University, 2002).

124. A. S. Verhulst, O. Liivak, M. H. Sherwood, H. M. Vieth, and I. L. Chuang, "Non-thermal nuclear magnetic resonance quantum computing using hyperpolarized xenon," Appl. Phys. Lett. **79,** 2480-2482 (2001).

125. M. H. Levitt, "Composite Pulses," Progress In Nuclear Magnetic Resonance Spectroscopy **18,** 61-122 (1986).

126. J. Wesenberg and K. Molmer, "Robust quantum gates and bus architecture for quantum computing with rare-earth-ion doped crystals.," quant-ph/ 0301036 (2003).

127. I. Roos, *Theoretical investigation of robust quantum computing in rare-earth-ion doped crystals*, (Lund Reports on Atomic Physics, LRAP-298, Diploma paper, Lund, Sweden, 2003).

128. M. D. Lukin and P. R. Hemmer, "Quantum entanglement via optical control of atom-atom interactions," Phys. Rev. Lett. **84,** 2818-2821 (2000).

129. K. Ichimura, "A simple frequency-domain quantum computer with ions in a crystal coupled to a cavity mode," Opt. Commun. **199,** 453-453 (2001).

130. M. S. Shahriar, P. R. Hemmer, S. Lloyd, P. S. Bhatia, and A. E. Craig, "Solid-state quantum computing using spectral holes," Phys. Rev. A **66,** art-032301 (2002).